Lithosphere-asthenosphere mixing in a transform-dominated late Paleozoic backarc basin: Implications for northern Cordilleran crustal growth and assembly

Stephen J. Piercey[1,*], Donald C. Murphy[2], and Robert A. Creaser[3]
[1]*Department of Earth Sciences, Memorial University of Newfoundland, 300 Prince Philip Drive, St. John's, Newfoundland and Labrador, A1B 3X5, Canada*
[2]*Yukon Geological Survey, P.O. Box 2703 (K-10), Whitehorse, Yukon, Y1A 2C6, Canada*
[3]*Department of Earth and Atmospheric Sciences, University of Alberta, 126 ESB, Edmonton, Alberta, T6G 1E3, Canada*

ABSTRACT

The Slide Mountain terrane is part of a North American Cordillera–long backarc basinal assemblage that developed between the ensialic arc terranes (Yukon-Tanana and affiliated pericratonic terranes) and the North American craton in the middle to late Paleozoic. The Slide Mountain basin started to open in the Late Devonian, and spreading continued through the late Paleozoic in an oblique (transform-dominated) manner such that the pericratonic terranes were translated into southerly latitudes. The basin closed, also in an oblique manner, by the Early Triassic, resulting in the reaccretion of the Yukon-Tanana terrane to the northwestern Laurentian margin. Both the opening and closing likely involved hundreds to possibly thousands of kilometers of intra-ocean and/or intra-arc strike-slip displacement, sinistral during the ocean's Late Devonian to mid-Permian opening and dextral during its Late Permian closing.

In southeastern Yukon, Canada, the Early Permian Slide Mountain terrane is dominated by mafic and ultramafic volcanic and plutonic rocks of the Campbell Range Formation. These rocks are narrowly distributed, for over 300 km, on either side of the Jules Creek–Vangorda fault, a fault that separates Slide Mountain terrane from Yukon-Tanana terrane. The Campbell Range basaltic volcanic and high-level intrusive rocks have geochemical and isotopic signatures that vary systematically across the Jules Creek–Vangorda fault: ocean-island basalt (OIB) and enriched mid-ocean ridge basalt (E-MORB) suites with lower εNd_t occur exclusively south of the fault, whereas north of the fault they have normal mid-ocean ridge basalt (N-MORB) and backarc basin basalt (BABB) signatures with higher εNd_t values. The εNd_t values are inversely correlated with Nb/Th_{pm} and Nb/La_{pm}, suggesting that the lower εNd_t values present in the E-MORB and OIB are mantle source features of these basalts and not due to continental crustal contamination. Isotopic and multi-element mixing calculations illustrate that the OIB-like basalts were derived primarily from enriched continental lithospheric mantle, whereas the N-MORB and BABB suites were sourced primarily from the upwelling backarc asthenospheric mantle; E-MORBs represent mixtures of depleted asthenospheric and enriched lithospheric mantle.

The geochemical and isotopic variations in the Campbell Range Formation across the Jules Creek–Vangorda fault is attributed to formation in different parts of an extending continental-backarc basin and then their subsequent juxtaposition by continued displacement along the fault.

Despite the juvenile isotopic signatures present in the Slide Mountain terrane, they occur as thin klippe atop rocks of recycled continental crustal affinity, suggesting that they were likely only minor contributors to Cordilleran crustal growth.

INTRODUCTION

The North American Cordillera has been held up as a model for the importance of accretionary processes in continental crustal growth and evolution (e.g., Monger and Nokleberg, 1996; Monger, 1997). During its evolution, the dominant mechanism of addition of juvenile crust to the orogen is thought to have been through the accretion of juvenile terranes to its external parts (Samson et al., 1989; Samson and Patchett, 1991). In contrast, the extensive subduction-generated magmatic arcs that developed at different times and places along the Cordilleran continental margin are largely considered to be localities where continental crustal recycling is the predominant process during crustal evolution (e.g., Hildreth and Moorbath, 1988). Geological, geochemical, and isotopic data from both the craton and the terranes with a peri-Laurentian geological history (e.g., Yukon-Tanana terrane) illustrates that abundant rocks formed within magmatic arcs that involved significant continental crustal recycling with little net addition of juvenile material to the continent (Creaser et al., 1997; Patchett and Gehrels, 1998; Piercey et al., 2003; Piercey et al., 2006).

During the late Paleozoic, the Cordilleran margin was characterized by a Sea of Japan–like backarc ocean (e.g., Slide Mountain terrane in Canada, Seventymile terrane in Alaska, and Golconda allochthon in western United States) separating a rifted continental arc fragment (Yukon-Tanana and affiliated pericratonic terranes) from the cratonic margin (Nelson, 1993; Creaser et al., 1999; Nelson et al., 2006). Continental margin backarc basins (e.g., Okinawa Trough and Sea of Japan) are settings where juvenile material is potentially added to continental margins by rifted margin magmatic processes (e.g., Pouclet et al., 1995; Shinjo, 1999), and if sufficiently long lived, and, importantly, preserved through subsequent tectonism, the remnants of backarc basins may represent a significant addition of juvenile material to

*Corresponding author email: spiercey@mun.ca

Geosphere; June 2012; v. 8; no. 3; p. 716–739; doi:10.1130/GES00757.1; 12 figures; 5 tables.
Received 17 October 2011 ♦ Revision received 22 March 2012 ♦ Accepted 26 March 2012 ♦ Published online 17 May 2012

continental margins (e.g., Patchett and Gehrels, 1998; Creaser et al., 1999; Piercey et al., 2006; van Staal, 2007).

The Slide Mountain and equivalent oceanic terranes extend for much of the length of the North American Cordillera, occurring in thrust sheets and klippe between the pericratonic late Paleozoic continental arc terranes and the North American continental margin (Figs. 1 and 2). The Slide Mountain ocean initially opened in the Late Devonian (~365 Ma) (Nelson, 1993), coeval with the onset of arc magmatism in the pericratonic terranes, and closed in the Late Permian by its westward subduction beneath the pericratonic terranes (Mortensen, 1992b; Creaser et al., 1999; Nelson et al., 2006; Piercey et al., 2006). Although much of the terrane was subducted in the Late Permian, some of the inboard portion of the terrane is preserved in British Columbia in the southern Canadian Cordillera and lies atop rocks of the North American craton (Keen Creek assemblage of Klepacki, 1985). Some of the outboard portions of the terrane are in stratigraphic and structural contact with rocks of the pericratonic Yukon-Tanana terrane in the northern Canadian Cordillera (Murphy et al., 2006), whereas some of the more juvenile portions of the terrane that formed in intra-oceanic settings are locally preserved throughout British Columbia and Yukon (Nelson, 1993; Ferri, 1997; Lapierre et al., 2003).

Mafic magmatism occurred intermittently in the Slide Mountain terrane. The oldest magmatic rocks in the terrane are Late Devonian to Early Mississippian in age (Klepacki, 1985; Struik and Orchard, 1985; Nelson, 1993). Little record of Carboniferous magmatism is preserved (e.g., Nelson, 1993); rocks of this age may have been largely subducted in the Late Permian. In the Late Pennsylvanian to Early Permian, however, the terrane exhibits a significant flare-up of magmatic activity from the southern Canadian Cordillera to Alaska (e.g., Klepacki, 1985; Struik and Orchard, 1985; Nelson, 1993; Roback et al., 1994; Ferri, 1997; Lapierre et al., 2003). Lower Permian basalt is the defining constituent of the Campbell Range Formation in southeastern Yukon (Mortensen, 1992a, 1992b; Plint and Gordon, 1997; Murphy and Piercey, 1999; Murphy et al., 2006). The geological, geochemical, and isotopic characteristics of the Campbell Range Formation are the subject of this paper.

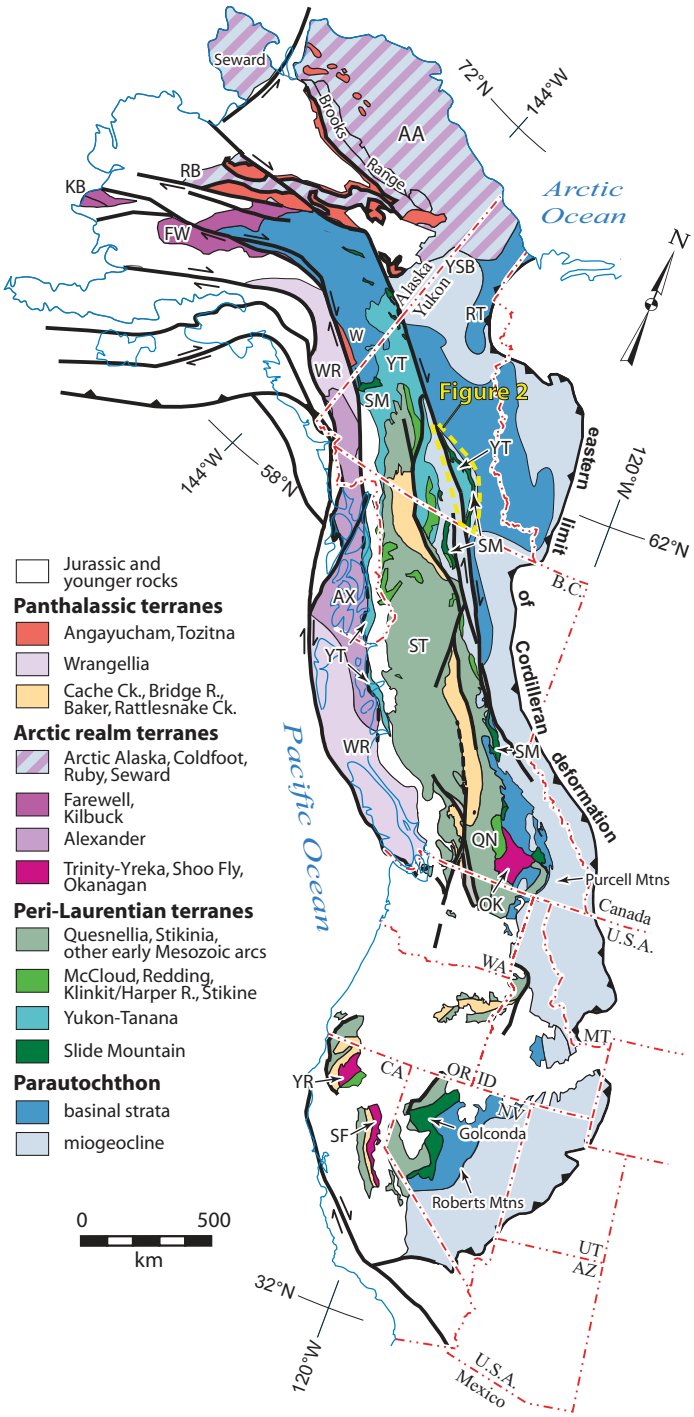

Figure 1. Terrane map of the North American Cordillera outlining the distribution of the Slide Mountain terrane in relation to other terranes of the Cordillera. Figure modified from Colpron and Nelson (2011).

Geochemical data for basalt of Slide Mountain terrane have been reported by Roback et al. (1994), Smith and Lambert (1995), Plint and Gordon (1997), Patchett and Gehrels (1998), Creaser et al. (1999), Dusel-Bacon and colleagues (Seventymile terrane, Dusel-Bacon and Cooper, 1999; Dusel-Bacon et al., 2006), Lapierre et al. (2003), Pigage (2004), and Piercey et al. (2006). As might be expected, most samples are normal mid-ocean ridge basalts (N-MORBs) with juvenile isotopic signatures (Piercey et al., 2006). However, enriched mid-ocean ridge basalts (E-MORBs) and rocks with geochemical signatures indistinguishable from those of modern plume-related environments have been documented in widely spaced localities (ocean-island basalts [OIBs]) (Lapierre et al., 2003; Piercey et al., 2006). These enriched

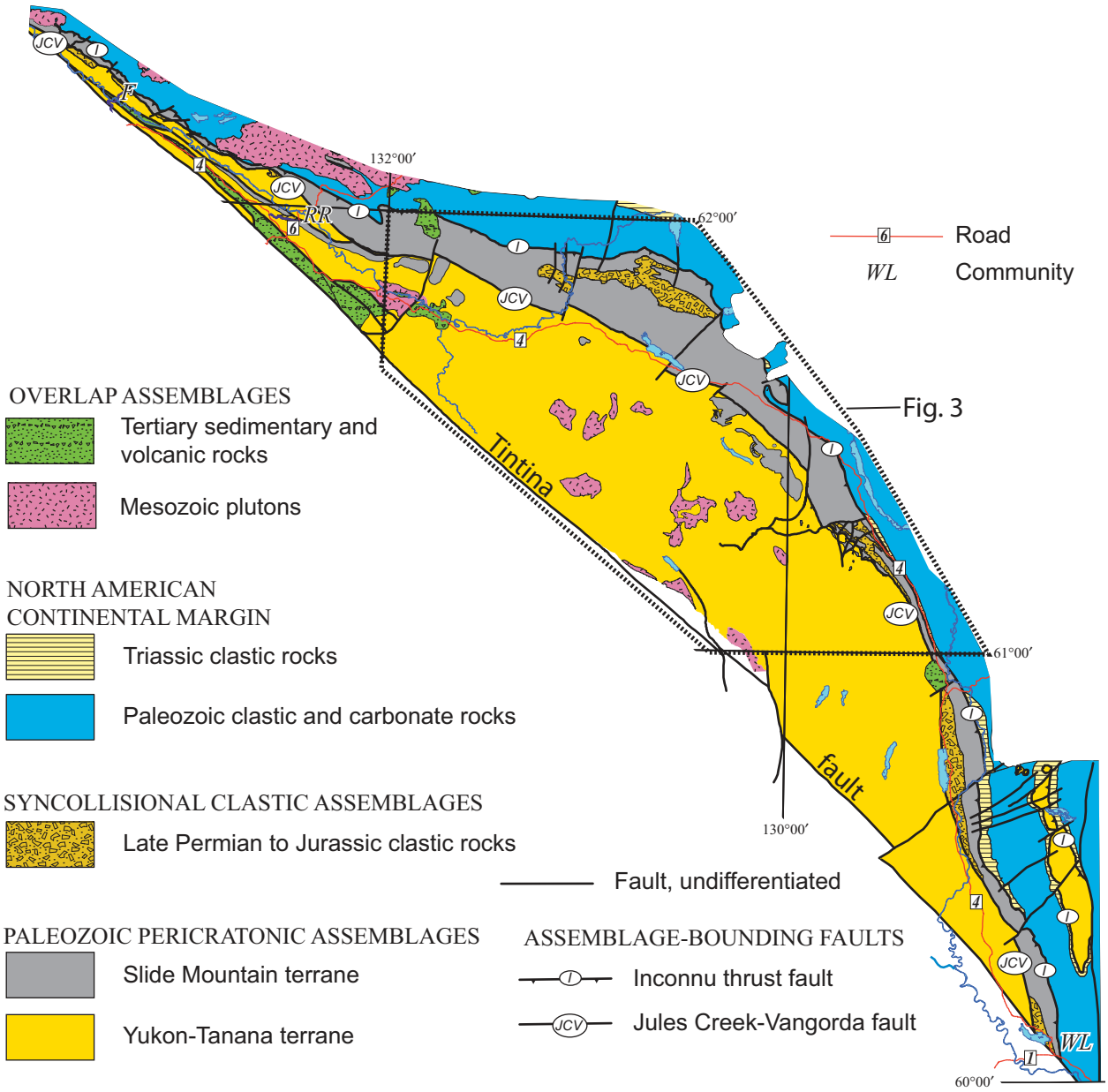

Figure 2. Distribution of Slide Mountain and Yukon-Tanana terranes and strata of the North American continental margin north of the Tintina fault, south-central Yukon. Pre–Early Permian strata of Slide Mountain terrane are in contact with Yukon-Tanana terrane across the Jules Creek–Vangorda fault (JCV); the Early Permian Campbell Range basalt of Slide Mountain terrane is in depositional contact with both pre–Early Permian strata of Slide Mountain terrane north of the JCV fault and Carboniferous rocks of Yukon-Tanana terrane south of the fault. The contact between the pericratonic terranes (Yukon-Tanana and Slide Mountain terranes) and strata of the North American continental margin is the post–Late Triassic Inconnu thrust (I). The outline of Figure 3, a more detailed map of the study area, is indicated by the dashed outline. Communities: *WL*—Watson Lake; *RR*—Ross River; *F*—Faro. Roads: *1*—Alaska Highway; *4*—Robert Campbell Highway; *6*—Canol Road.

signatures have led Lapierre et al. (2003) to infer widespread influence of mantle plumes in the generation of Slide Mountain terrane basalts.

One little discussed aspect of the evolution of the paired arc (Yukon-Tanana and other pericratonic terranes)–backarc ocean (Slide Mountain terrane) system is the requirement for substantial latitudinal displacement to be embedded within the system, as strike-slip faults within the arc and/or as oceanic transform faults. Numerous lines of evidence suggest that Yukon-Tanana terrane, the largest pericratonic arc terrane, was a part of northwestern Laurentia before the onset of Late Devonian backarc rifting (Colpron et al., 2006, 2007; Nelson et al., 2006; Piercey and Colpron, 2009); however, by the mid-Permian, it and companion terranes were at sufficiently southerly latitudes for limestone

containing the McCloud fusilinid fauna to have been deposited on them (Miller, 1988; Stevens, 1995; Belasky et al., 2002; Nelson et al., 2006). Because species of the McCloud fauna occur on the craton only as far north as the latitude of Texas (Ross, 1969), there is an implication that the Slide Mountain ocean had significant strike-slip displacement, before final re-attachment to northwestern Laurentia by the Triassic (Beranek et al., 2010). At present, however, the details of this displacement history are not completely understood.

In this paper, we document the geological characteristics and setting of the Campbell Range Formation of Slide Mountain terrane in southeastern Yukon and present new geochemical and isotopic data from the terrane. We use these data to support an interpretation that the range of geochemical signatures that we and others have documented has more to do with the compositional diversity of the source regions for the basalt rather than the influence of an active mantle plume. We argue that the plume-like attributes of the basalts were likely inherited from a lithospheric mantle. Furthermore, we attribute the formation and juxtaposition of the different geochemical domains to an origin along a "leaky" transform fault, the Jules Creek–Vangorda fault. The Jules Creek–Vangorda fault is inferred to be one of a system of sinistral strike-slip faults along which the plate containing the ensialic arc terrane was transported to more southerly latitudes in which the McCloud fauna existed.

Our study points out that although the record of the continental margin and pericratonic ensialic arcs such as represented by Yukon-Tanana terrane is predominantly one of continental arc magmatism and attendant recycling of ancient crustal material (Mortensen, 1992b; Piercey et al., 2006; Piercey and Colpron, 2009), there are juvenile backarc basin rocks within the Slide Mountain terrane. We will evaluate what role this juvenile magmatism has played in Cordilleran crustal growth during the late Paleozoic and whether or not it has been an important contributor to net crustal growth of this orogen.

SLIDE MOUNTAIN TERRANE IN SOUTHEASTERN YUKON

In southeastern Yukon, the Slide Mountain terrane occurs primarily in a narrow, elongate and arcuate belt extending for over 300 km between Faro and the British Columbia–Yukon border south of Watson Lake (Figs. 2–4). It consists of a Carboniferous sediment-dominated assemblage (Fortin Creek group of Murphy et al., 2006; Mount Aho and Rose Mountain formations of Pigage, 2004) and a Lower Permian sequence of basalt, chert, and argillite, the Campbell Range Formation. Mafic and ultramafic intrusions, probably comagmatic with the basalt, are also significant components of the terrane.

The Fortin Creek group is composed primarily of Carboniferous to Lower Permian carbonaceous phyllite, chert, chert-pebble conglomerate, lesser quartzofeldspathic wacke and limestone, and rare felsic and mafic metavolcanic rocks. Metavolcanic rocks have alkalic (felsic) and N-MORB (mafic) affinities suggesting a rift setting (Murphy et al., 2006). The Fortin Creek group is increasingly more deformed to the north, where it is stratigraphically overlain by a conglomerate containing clasts of the highly strained Fortin Creek group. The precise age of this conglomerate at this locality is not known, but it is Middle Triassic or younger (Beranek, 2009). The zone of intense deformation in the Fortin Creek group therefore must be Late Permian to Early Triassic in age, and is inferred to be part of the subduction complex at which the remainder of the Slide Mountain ocean was consumed.

The Campbell Range Formation consists of weakly deformed and relatively well preserved basalt and chert. Basalt comprises black to dark-green massive and pillowed lava flows, interflow and interpillow hyaloclastite, and brecciated fragmental varieties (Murphy and Piercey, 1999; Murphy et al., 2002). Epidote-quartz-hematite alteration is common. Primary igneous mineralogy is generally well preserved with phenocrysts and microphenocrysts of olivine, clinopyroxene, and plagioclase still present, even in proximity to hydrothermal mineralization (e.g., Ice Deposit, Mann and Mortensen, 2000). Locally, primary igneous minerals are pseudomorphed by very low grade secondary minerals.

Chert, argillite, and lesser limestone are locally important in the Campbell Range Formation. Maroon, pink, and green chert commonly form ribbons 10–30 cm in thickness and are typically interlayered with argillite (Murphy et al., 2002). These sedimentary members are often foliated and folded to a greater extent than the surrounding basaltic rocks (Murphy et al., 2002).

Mafic and ultramafic plutonic rocks are spatially associated with the Campbell Range Formation. These comprise gabbro, leucogabbro, pyroxenite, and variably serpentinized peridotite, forming bodies ranging in size from a few hundred square meters to over 2 km^2 (Figs. 2 and 3; Murphy et al., 2002, 2006). The spatial association of the mafic and ultramafic plutonic rocks with the Campbell Range basalt implies a genetic relationship, and they are likely the coeval subvolcanic roots to the basalt (Figs. 2 and 3; Murphy et al., 2002, 2006).

The Campbell Range Formation is constrained by both fossil and radiometric ages to be Early Permian. In the Finlayson Lake district, chert in the lower Campbell Range Formation has yielded early Pennsylvanian to Early Permian radiolaria (Harms in Plint and Gordon, 1997), yet basalt locally overlies the Money Creek Formation, a unit that unconformably overlies limestone with Late Pennsylvanian to Early Permian fauna (Figs. 2–4). On strike to the west near Faro (Fig. 2), chert of the Campbell Range Formation contains Early Permian (Asselian–Sakmarian) radiolaria (Pigage, 2004). Two U-Pb zircon ages of ~274 Ma (Early Permian) have been obtained from leucogabbro that crosscuts the Campbell Range basalt (Mortensen, 1992a; Murphy et al., 2006).

The Slide Mountain terrane in southeastern Yukon lies primarily between the North American continental margin sequence and the Yukon-Tanana terrane, an ensialic late Paleozoic arc terrane with a pre–Late Devonian basement of inferred northwestern North American affinity (Figs. 2–4; Colpron et al., 2006; Nelson et al., 2006; Piercey et al., 2006; Piercey and Colpron, 2009). Along their north and eastern contacts, the Slide Mountain and Yukon-Tanana terrane lies in fault contact with North American continental margin rocks along the Jura-Cretaceous Inconnu thrust fault (Figs. 2 and 3; Murphy et al., 2006). To the south and west, the relationship between rocks of Slide Mountain and Yukon-Tanana terranes is more complex. The Jules Creek–Vangorda fault separates the Devono-Carboniferous rocks of Slide Mountain terrane (Fortin Creek group and equivalent rocks) from coeval rocks of the Yukon-Tanana terrane (Money Creek Formation and Wolverine Lake group); however, the basalt- and chert-dominated Lower Permian part of Slide Mountain terrane, the Campbell Range Formation, lies in depositional contact on older rocks on both sides of the fault (Figs. 2 and 3; Murphy et al., 2006). The unfaulted nature of the contact between the Campbell Range Formation of Slide Mountain terrane and rocks of Yukon-Tanana terrane is prima facie evidence that the two terranes evolved together in the same geodynamic setting in the Early Permian. The Early Permian rocks of the Campbell Range Formation are coeval with arc volcanic rocks of the Klinkit Group located south of the Tintina fault near the British Columbia–Yukon border (Fig. 1; Simard et al., 2003).

The Jules Creek–Vangorda fault is an important structure that contains significant Campbell Range basalt and, importantly, affiliated plutonic rocks, within only a few kilometers of the

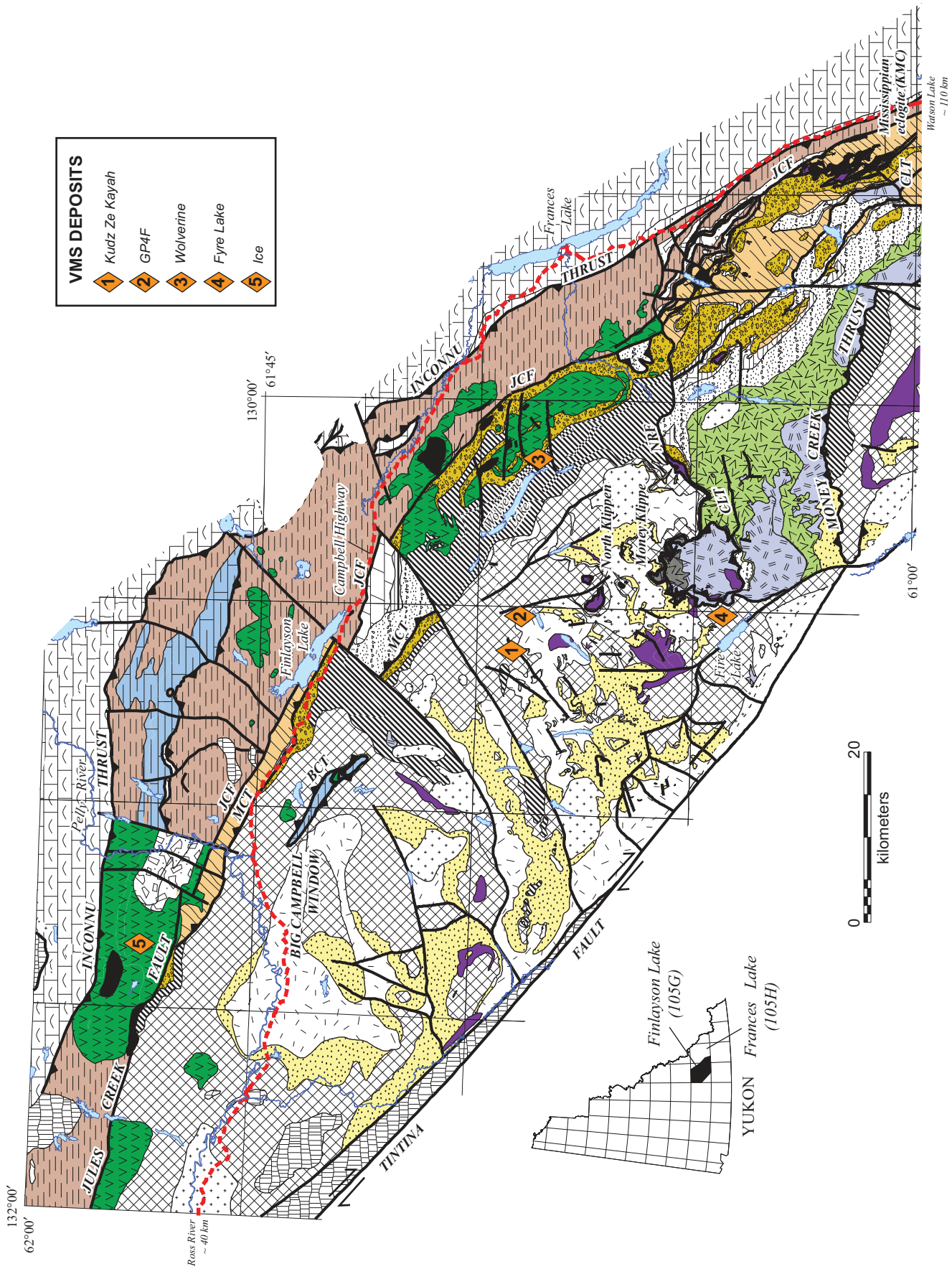

Figure 3 (*legend on following page*). Geological map of the Campbell Range Formation and associated rocks of the Finlayson Lake region, Yukon. Map modified from Murphy et al. (2006).

Figure 3 (*legend*).

fault for a strike length of over 300 km. Furthermore, the Campbell Range Formation occurs at about the same elevation on both sides of the fault, implying a strike-slip origin with sinistral motion but with a likely dextral reactivation in the late Paleozoic (see discussion).

GEOCHEMISTRY AND RADIOGENIC ISOTOPES

Sampling and Analytical Methods

Samples of basalt from the Campbell Range Formation and coeval subvolcanic intrusions were collected during regional mapping in the 1998 and 2001 field seasons. Samples from the 1998 field season were analyzed at the Geological Survey of Canada, Ottawa, Canada (Table 1). Samples were analyzed using fused bead X-ray fluorescence (XRF) for most of the major elements. Water (H_2O_T) and CO_{2T} were analyzed by infrared spectroscopy, and FeO was analyzed by modified Wilson titration. Trace elements were analyzed by combined inductively coupled plasma–emission spectrometry (ICP-ES: Ba, La, Pb, Sc, Sr, V, Y, and Yb) and mass spectrometry (ICP-MS: remaining rare-earth elements [REE], Cs, Rb, Th, U, Ga, Hf, and Ta). Analytical precision calculated from repeat analyses of internal basaltic reference materials (Piercey et al., 2004) is given as percent relative standard deviation (%RSD = 100*standard deviation/mean), and yielded values of: 0.43%–6.52% for the major elements, 0.72%–8.80% for the transition elements (V, Ni, Cr, Co), 2.21%–5.92% for the high field strength elements (HFSEs) (Nb, Zr, Hf, Y, Sc, and Ga), 2.35%–6.96% for the low field strength elements (LFSEs) (Cs, Rb, Th and U), but slightly higher for Ba and Sr (1.49%–15.75%), and 2.15%–6.47% for the REEs.

Samples from the 2001 field season were analyzed by XRF for their major elements (on fused discs), selected trace elements (on pressed pellets: Ni, Co, Cr, V, Cu, Pb, Zn, As, Ga, Sr, Rb, and Ba), and loss on ignition (LOI) at the University of Western Ontario (UWO), London, Ontario, Canada, following the methods outlined in Wu (1984), Mata et al. (1998), and Young (2002). The remaining trace elements and REEs were analyzed by ICP-ES (S, Sc, Mo, W, Cd, Be, and Li) and ICP-MS (Nb, Ta, Zr, Hf, Y, Cs, Th, U, La, Ce, Pr, Nd, Sm, Eu, Gd, Tb, Dy, Ho, Er, Tm, Yb, and Lu) at the Ontario Geoscience Laboratories, Sudbury, Ontario, Canada, using a closed-beaker multi-acid digestion prior to analysis (Burnham et al., 2002; Burnham and Schweyer, 2004). Precision for XRF analysis, based on replicate analyses of reference materials, is less than ±2% for major elements (±5% for P_2O_5 and Na_2O) and ±5%–10% for trace elements (Wu, 1984; Mata et al., 1998; Young, 2002). Accuracy for XRF analyses based on analyses of U.S. Geological Survey

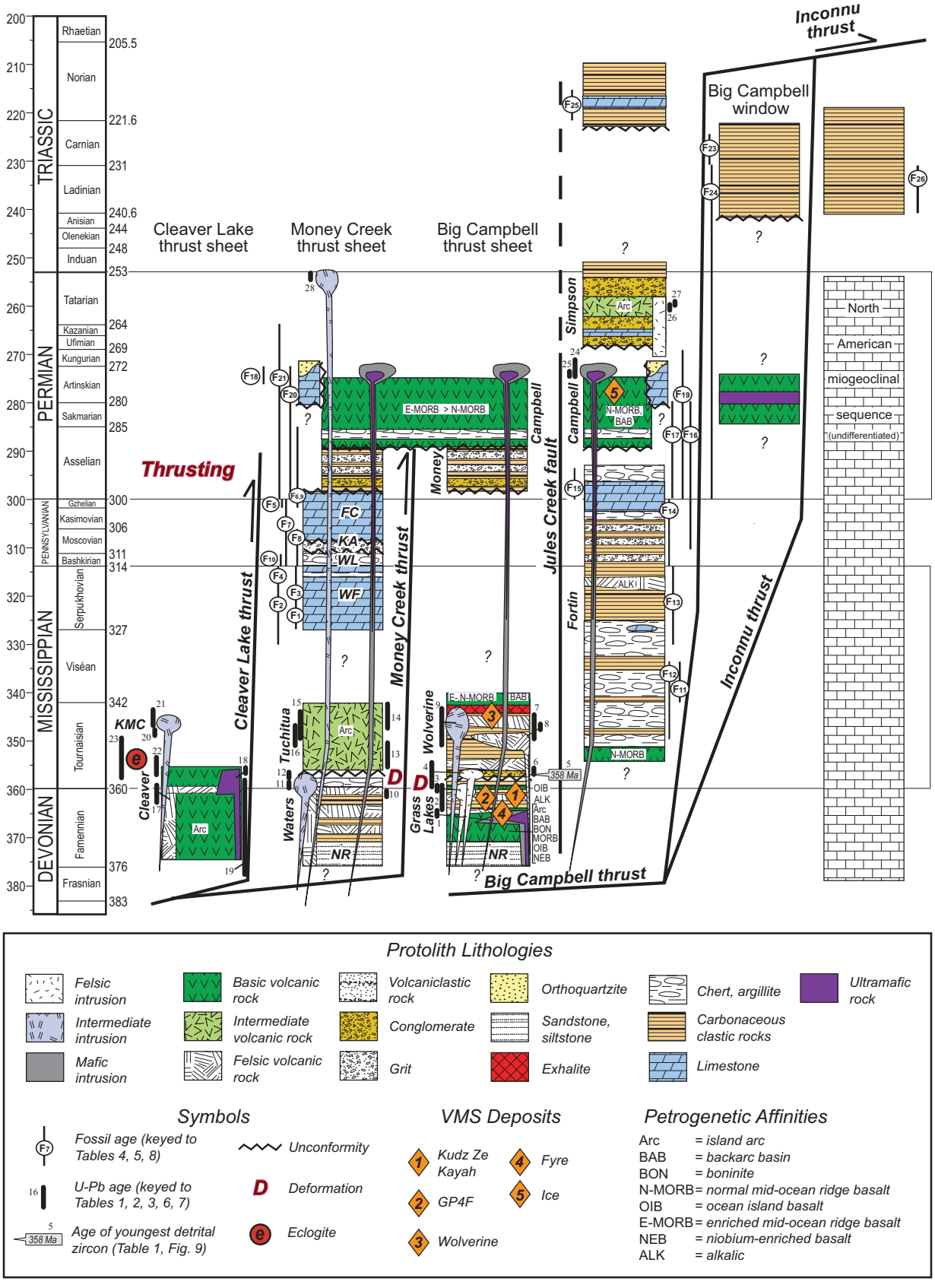

Figure 4. Stratigraphic sections for the Finlayson Lake region Yukon with relationship of the Campbell Range Formation to other rocks of the Yukon-Tanana terrane. From Murphy et al. (2006).

TABLE 1. WHOLE-ROCK GEOCHEMICAL DATA FOR BASALTIC ROCKS FROM THE CAMPBELL RANGE FORMATION

Sample name	P98-59A	P98-59B	P98-60	P98-77	P98-63	P98-78	P98-87	01CR-113	01MC-007	01MC-008	01MC-114	P98-61
Easting	437301	437301	437520	434104	439917	443131	443604	420588	375294	375453	416443	437083
Northing	6815041	6815041	6815390	6819048	6816364	6816509	6812956	6848191	6864720	6864823	6849824	6815615
Rock type	MB	MG	DB	MB	PB	MG	MG	MB	MB	MB	MB	MB
Affinity	OIB	OIB	OIB	OIB	N-MORB (S)	N-MORB (S)	N-MORB (S)	N-MORB (N)	N-MORB (N)	N-MORB (N)	N-MORB (N)	E-MORB
SiO_2 (wt%)	42.80	46.60	46.20	48.40	51.30	48.90	47.20	49.15	50.13	48.87	49.33	50.40
TiO_2	1.90	2.19	1.51	2.02	1.54	3.23	1.36	1.16	1.04	0.94	1.28	1.80
Al_2O_3	15.60	15.70	13.10	16.80	13.30	12.30	15.10	14.73	14.62	14.28	15.06	13.70
Fe_2O_3T	9.00	9.30	8.80	8.40	11.30	15.10	12.20	10.54	11.14	10.36	9.50	11.60
Fe_2O_3	5.00	4.20	1.20	3.00	2.70	2.60	3.10	–	–	–	–	4.10
FeO	3.60	4.60	6.80	4.90	7.70	11.30	8.20	–	–	–	–	6.70
MnO	0.16	0.15	0.16	0.12	0.19	0.22	0.18	0.20	0.15	0.16	0.16	0.16
MgO	4.55	6.65	14.20	4.00	6.96	5.47	8.72	7.20	7.09	7.78	6.53	6.36
CaO	13.89	11.23	9.10	9.85	9.98	9.96	9.53	8.94	7.00	9.00	9.28	10.46
Na_2O	3.60	3.80	1.10	3.00	3.60	2.70	3.10	0.10	0.45	1.18	0.58	3.80
K_2O	0.96	0.49	1.70	3.43	0.12	0.22	0.04	4.13	4.58	2.78	3.91	0.10
P_2O_5	0.37	0.43	0.36	0.55	0.13	0.42	0.10	0.11	0.10	0.13	0.11	0.18
H_2O	2.90	3.00	4.90	2.60	3.10	2.70	3.90	–	–	–	–	2.60
CO_2	5.30	1.50	0.20	1.90	0.10	0.20	0.10	–	–	–	–	0.50
LOI	–	–	–	–	–	–	–	2.46	2.00	2.92	2.32	–
Total	101.03	101.04	101.33	101.07	101.62	101.42	101.53	98.73	98.28	98.39	98.06	101.66
S (ppm)	–	–	–	–	–	–	–	788	360	477	472	–
Cr	154	219	858	209	208	108	282	280	111	172	191	161
Ni	70	77	412	86	53	40	73	120	60	64	85	50
Co	37	34	48	32	42	40	51	38	45	42	39	43
Sc	27	32	26	28	33	39	47	36	40	42	36	43
V	230	294	208	206	327	423	272	276	279	249	247	291
Cu	38	55	50	51	55	27	114	55	65	32	59	29
Pb	<1	2	<1	2	<1	1	<1	<1	<1	<1	<1	<1
Zn	70	50	53	54	67	109	74	81	77	83	65	73
Rb	18.0	10.0	39.0	89.0	1.3	4.1	0.3	6.2	16.8	35.0	23.1	1.5
Cs	0.61	0.22	1.20	3.00	0.09	0.12	0.04	0.68	0.71	0.98	0.26	0.19
Ba	158	298	1067	1431	55	132	48	258	316	226	268	56
Sr	148	226	49	542	24	147	289	278	50	53	240	122
Ga	17.0	19.0	14.0	18.0	16.0	21.0	16.0	17.5	11.9	13.8	13.3	17.0
Ta	2.50	3.70	3.20	3.60	0.55	0.91	0.54	<0.3	<0.3	<0.3	<0.3	0.90
Nb	42.0	61.0	55.0	61.0	2.3	9.1	4.7	1.6	0.9	3.7	1.9	11.0
Hf	2.90	3.50	2.70	3.30	2.50	6.20	1.70	2.30	1.84	1.66	2.61	2.50
Zr	121.0	146.0	119.0	143.0	96.0	253.0	59.0	74.1	72.3	61.9	86.2	93.0
Y	31.0	30.0	22.0	27.0	33.0	77.0	32.0	31.1	32.9	30.8	32.7	37.0
Th	3.10	4.50	4.20	4.40	0.18	0.50	0.31	0.17	0.08	0.10	0.16	0.76
U	0.75	1.10	0.93	0.68	0.10	0.21	0.08	0.10	0.03	0.06	0.04	0.30
La	22.00	32.00	27.00	31.00	3.70	9.70	4.20	3.13	1.83	2.86	2.85	7.20
Ce	45.00	61.00	53.00	61.00	11.00	29.00	11.00	9.49	6.07	7.31	9.43	18.00
Pr	5.20	7.00	5.90	7.00	2.10	4.60	1.70	1.62	1.18	1.26	1.68	2.50
Nd	21.00	28.00	23.00	28.00	11.00	24.00	9.30	8.35	6.81	6.85	9.03	13.00
Sm	5.70	6.80	5.20	6.20	3.60	8.80	3.40	2.96	2.60	2.34	3.19	4.60
Eu	1.70	2.10	1.50	1.70	1.00	2.50	1.30	1.17	1.00	1.09	1.29	1.60
Gd	5.50	6.10	4.30	5.40	5.00	11.00	4.20	4.10	3.85	3.62	4.40	5.50
Tb	0.92	0.95	0.68	0.85	0.87	2.00	0.79	0.74	0.72	0.65	0.79	0.99
Dy	5.40	5.40	3.90	4.70	5.60	12.00	5.00	4.86	4.77	4.41	5.26	6.00
Ho	1.10	1.00	0.75	0.90	1.20	2.60	1.10	1.07	1.08	0.98	1.19	1.20
Er	2.80	2.60	1.80	2.30	3.40	7.20	2.80	3.18	3.08	2.86	3.28	3.30
Tm	0.40	0.38	0.28	0.32	0.52	1.10	0.40	0.46	0.45	0.42	0.49	0.49
Yb	2.60	2.40	1.80	2.00	3.60	7.30	2.70	2.96	2.80	2.62	3.03	3.20
Lu	0.36	0.34	0.26	0.30	0.52	1.10	0.39	0.46	0.44	0.40	0.47	0.45

(*continued*)

standard basalt BHVO-1 as an unknown is typically less than ±10%, with many elements ±5% of recommended values (Mata et al., 1998). Precision and accuracy for trace element analyses by ICP-ES and ICP-MS at the Ontario Geoscience Laboratories is <7% RSD for precision, and below 8% RSD for accuracy (except Nb = 9.8% RSD and Pr = 12.3% RSD; Lightfoot and Farrow, 2002; Burnham and Schweyer, 2004). The geochemical data are presented in Table 1; key major and trace element ratios are presented in Table 2.

Thirteen samples were analyzed for Sm-Nd isotopic compositions at the University of Alberta Radiogenic Isotope Facility. Samples were analyzed by thermal ionization mass spectrometry (TIMS) and multicollector–inductively coupled plasma–mass spectrometry (MC-ICP-MS), following the methods of Creaser et al. (1997) and Unterschutz et al. (2002). Values for the Geological Survey of Japan (GSJ) Shin Etsu Nd isotope standard yielded an average $^{143}Nd/^{144}Nd$ = 0.512107 with an analytical uncertainty of ±0.000012 (1σ), which is interpreted to be the minimum uncertainty estimate of the $^{143}Nd/^{144}Nd$ for any particular sample (Creaser et al., 1997). Neodymium isotope data are presented relative to a value of $^{143}Nd/^{144}Nd$ = 0.512107 for the Geological Survey of Japan Shin Etsu Nd standard, which is equivalent to 0.511850 for the La Jolla standard (Tanaka et al., 2000). Initial $^{143}Nd/^{144}Nd$ ratios and εNd were calculated at 274 Ma, the approximate ages of the rocks from the Campbell Range Formation (Mortensen, 1992a; Murphy et al., 2006). Values used for the chondrite uniform reservoir (CHUR) to obtain initial $^{143}Nd/^{144}Nd$ and εNd values are $^{147}Sm/^{144}Nd$ = 0.196593 and $^{143}Nd/^{144}Nd$ = 0.512638 (Hamilton et al., 1983). Depleted mantle model ages are shown for rocks with $^{147}Sm/^{143}Nd$ <0.16 and calculated from model $^{147}Sm/^{143}Nd$ and $^{143}Nd/^{144}Nd$ values

TABLE 1. WHOLE-ROCK GEOCHEMICAL DATA FOR BASALTIC ROCKS FROM THE CAMPBELL RANGE FORMATION (*continued*)

Sample name	P98-66	P98-72	P98-59	P98-62	P98-88	P98-95	98DM-151	98DM-158	98DM-162	01MC-013	01MC-116
Easting	437917	436748	437301	437287	443591	445201	441470	440505	441978	377056	417062
Northing	6815791	6814391	6815041	6816031	6812439	6808759	6814798	6811963	6812269	6866244	6848003
Rock type	PB	MB	MB	MB	MB	PB	MB	MB	PB	MB	MB
Affinity	E-MORB	E-MORB	E-MORB	E-MORB	E-MORB	E-MORB	E-MORB	E-MORB	E-MORB	BABB	BABB
SiO_2 (wt%)	50.60	46.20	47.00	49.60	49.20	49.50	48.70	48.20	51.10	51.17	48.15
TiO_2	1.38	1.46	1.90	1.88	1.48	1.12	1.26	1.42	2.00	0.60	1.21
Al_2O_3	14.00	13.90	14.20	14.40	14.50	15.20	14.30	16.10	13.10	16.36	15.60
Fe_2O_3T	9.90	10.00	10.90	11.50	10.90	9.60	10.30	9.90	12.30	9.76	11.15
Fe_2O_3	1.50	5.50	1.60	3.30	1.60	2.60	1.80	3.30	2.60	–	–
FeO	7.60	4.10	8.30	7.40	8.30	6.30	7.60	6.00	8.70	–	–
MnO	0.14	0.16	0.18	0.14	0.19	0.14	0.17	0.14	0.19	0.16	0.14
MgO	7.26	5.50	6.49	5.39	6.50	7.28	8.63	7.37	6.16	6.67	5.06
CaO	10.40	14.60	7.89	12.29	10.14	11.02	10.69	10.16	9.15	5.49	10.17
Na_2O	4.00	3.30	3.60	3.20	4.10	3.50	2.90	2.30	3.90	0.34	0.06
K_2O	0.22	0.25	0.39	0.16	0.18	0.34	0.42	1.75	0.41	4.83	4.49
P_2O_5	0.13	0.16	0.22	0.22	0.14	0.10	0.12	0.15	0.23	0.05	0.12
H_2O	3.00	2.20	4.10	2.10	2.90	2.70	3.70	3.00	2.50	–	–
CO_2	0.50	3.30	4.50	0.30	1.10	0.50	0.10	0.40	0.30	–	–
LOI	–	–	–	–	–	–	–	–	–	3.06	2.53
Total	101.53	101.03	101.37	101.18	101.33	101.00	101.29	100.89	101.34	98.48	98.69
S (ppm)	–	–	–	–	–	–	–	–	–	298	521
Cr	317	168	68	85	260	340	316	279	38	22	51
Ni	75	81	46	51	66	120	89	80	39	22	47
Co	50	45	50	49	51	46	47	45	51	36	39
Sc	41	40	39	41	41	35	38	38	39	36	34
V	261	254	290	340	290	230	266	257	331	261	294
Cu	94	43	100	85	85	86	91	89	83	69	37
Pb	<1	1	<1	<1	<1	<1	<1	<1	<1	<2	<2
Zn	55	50	86	68	68	54	46	46	71	55	100
Rb	4.1	5.2	8.4	2.9	4.7	8.2	9.4	37.0	9.2	10.5	5.2
Cs	0.17	0.19	0.34	0.16	0.24	0.24	0.51	0.55	0.15	0.22	0.45
Ba	61	52	120	120	310	30	97	350	120	79	96
Sr	41	145	37	230	150	76	51	220	81	144	66
Ga	14.0	16.0	17.0	19.0	15.0	15.0	17.0	18.0	15.0	14.9	18.3
Ta	0.76	0.80	0.90	0.90	0.50	0.40	0.75	0.90	1.30	<0.3	<0.3
Nb	6.7	9.7	15.0	15.0	8.1	6.8	8.0	9.8	17.0	0.9	1.9
Hf	1.90	2.20	2.60	2.60	2.00	1.50	1.60	2.30	2.50	1.45	2.40
Zr	71.0	88.0	110.0	97.0	76.0	53.0	50.0	80.0	83.0	48.5	78.3
Y	30.0	29.0	31.0	35.0	30.0	25.0	30.0	27.0	36.0	22.0	33.1
Th	0.46	0.67	1.00	1.10	0.56	0.48	0.51	0.73	1.20	0.42	0.50
U	0.15	0.50	0.35	0.49	0.14	0.14	0.15	0.24	0.38	0.18	0.14
La	4.70	6.10	9.70	12.00	6.00	4.90	5.20	7.40	13.00	2.67	5.63
Ce	12.00	16.00	25.00	26.00	15.00	12.00	13.00	17.00	29.00	6.89	14.44
Pr	1.80	2.30	3.50	3.60	2.30	1.70	1.80	2.40	3.70	1.09	2.23
Nd	9.30	11.00	17.00	17.00	12.00	8.70	9.40	12.00	19.00	5.66	11.22
Sm	3.30	3.80	4.30	4.60	3.30	2.60	3.00	3.30	4.40	1.99	3.35
Eu	1.10	1.30	1.30	1.70	1.30	1.00	0.97	1.10	1.40	0.81	1.28
Gd	4.10	4.40	5.40	5.70	4.60	3.60	3.80	4.10	5.40	2.76	4.36
Tb	0.74	0.77	0.86	0.95	0.77	0.61	0.68	0.67	0.90	0.48	0.80
Dy	4.70	4.60	5.30	5.70	4.80	3.70	4.30	4.30	5.50	3.27	5.04
Ho	0.99	0.97	1.10	1.20	1.00	0.82	0.93	0.93	1.20	0.71	1.13
Er	2.60	2.60	2.90	3.30	2.80	2.30	2.50	2.40	3.20	2.09	3.19
Tm	0.40	0.38	0.45	0.51	0.44	0.35	0.38	0.38	0.48	0.32	0.44
Yb	2.70	2.50	2.70	3.00	2.90	2.30	2.60	2.60	3.10	2.12	3.08
Lu	0.40	0.37	0.37	0.43	0.40	0.32	0.39	0.38	0.45	0.31	0.47

Note: All samples are from Universal Transverse Mercator (UTM) Zone 9, North American Datum 1983. Abbreviations: DB—diabase; MB—massive basalt; MG—massive greenstone; N-MORB—normal mid-ocean ridge basalt; OIB—ocean-island basalt; PB—pillow basalt; N—north of Jules Creek-Vangorda Fault; S—south of Jules Creek-Vangorda Fault.

of 0.2137 and 0.513163, respectively (Goldstein et al., 1984). Results for the Nd isotopic analyses are presented in Table 3.

Alteration-Metamorphism and Element Mobility

During the course of this study, samples were selected to provide the best possible representation of samples for the regional distribution of the Campbell Range Formation. Attempts were made to sample the freshest samples without veins and visible hydrothermal alteration; however, in some cases samples do exhibit replacement of primary minerals by secondary hydrothermal and/or metamorphic assemblages (see descriptions of the Campbell Range basalts above). The presence of secondary chlorite-epidote-sericite ± minor carbonate alteration and metamorphic minerals implies that some of the Campbell Range belt basalts have experienced greenschist-grade metamorphic conditions. These conditions imply that most of the major elements, except Al_2O_3, TiO_2, and P_2O_5 (e.g., Whitford et al., 1989), were likely mobile during the alteration. Similarly, it is likely that the low field strength elements Cs, Rb, Ba, and Sr were likely mobile during alteration and metamorphism (e.g., MacLean, 1990). In contrast, the REEs, transition elements (Cr, Ni, Sc, and V), HFSEs, Th, and U were likely immobile during hydrothermal alteration and metamorphism (e.g., Lesher et al., 1986; MacLean, 1990; Jenner, 1996). To semiquantitatively test whether the latter elements have remained immobile, we have plotted a selection of elements and key element ratios against the Al_2O_3/Na_2O alteration index (Fig. 5; Spitz and Darling, 1978). From Figure 5, no systematic relationship between these element ratios and the degree of alteration and metamorphism is apparent, suggesting that they have remained immobile during these processes.

Analytical Results

The basaltic rocks from the Campbell Range Formation can be separated into four suites based on their immobile incompatible-element systematics, and patterns on primitive mantle– and chondrite-normalized trace element plots (Figs. 6–10). The following subsections outline the geochemical and Nd-isotopic attributes of each suite.

OIB Suite

Rocks of the OIB suite have alkalic basaltic affinities with basaltic Zr/TiO_2 values and Nb/Y >0.7 (Fig. 6A), broadly coincident with their SiO_2 contents (Table 1). The suite has relatively elevated TiO_2 contents (1.51%–2.19%; Table 1; Fig. 6), and low Al_2O_3/TiO_2 ratios (7–9), similar to modern E-MORB and OIB (Al_2O_3/TiO_2 ~5–9.5; Fig. 6; Sun and McDonough, 1989). The OIB suite contains higher HFSE and REE

TABLE 2. KEY MAJOR AND TRACE ELEMENT RATIOS FOR BASALTIC ROCKS FROM THE CAMPBELL RANGE FORMATION

Sample name	P98-59A	P98-59B	P98-60	P98-77	P98-63	P98-78	P98-87	01CR-113	01MC-007	01MC-008	01MC-114	P98-61
Rock type	MB	MG	DB	MB	PB	MG	MG	MB	MB	MB	MB	MB
Affinity	OIB	OIB	OIB	OIB	N-MORB (S)	N-MORB (S)	N-MORB (S)	N-MORB (N)	N-MORB (N)	N-MORB (N)	N-MORB (N)	E-MORB
Al_2O_3/Na_2O	4	4	12	6	4	5	5	141	33	12	26	4
Al_2O_3/TiO_2	8	7	9	8	9	4	11	13	14	15	12	8
Ti/V	50	45	44	59	28	46	30	25	22	23	31	37
Ti/Zr_{pm}	0.81	0.77	0.65	0.73	0.83	0.66	1.19	0.81	0.74	0.78	0.76	1.00
Nb/La_{pm}	1.8	1.8	2.0	1.9	0.6	0.9	1.1	0.5	0.5	1.3	0.7	1.5
Nb/Th_{pm}	1.6	1.6	1.6	1.7	1.5	2.2	1.8	1.2	1.3	4.5	1.4	1.7
Nb/Y	1.35	2.03	2.50	2.26	0.07	0.12	0.15	0.05	0.03	0.12	0.06	0.30
Nb/U	56.0	55.5	59.1	89.7	23.0	43.3	58.8	16.4	30.0	62.3	48.3	36.7
Nb/Yb	16.2	25.4	30.6	30.5	0.6	1.2	1.7	0.6	0.3	1.4	0.6	3.4
Zr/Y	22.0	23.9	27.7	26.5	19.2	23.0	14.0	18.1	18.8	17.1	19.6	16.9
Zr/Nb	2.9	2.4	2.2	2.3	41.7	27.8	12.6	45.2	80.3	16.6	44.7	8.5
Zr/Yb	46.5	60.8	66.1	71.5	26.7	34.7	21.9	25.0	25.8	23.6	28.4	29.1
Hf/Sm	0.51	0.51	0.52	0.53	0.69	0.70	0.50	0.78	0.71	0.71	0.82	0.54
La/Sm	3.9	4.7	5.2	5.0	1.0	1.1	1.2	1.1	0.7	1.2	0.9	1.6
Sm/Yb	1.1	1.5	1.5	1.7	0.7	0.8	0.6	0.8	0.7	0.6	0.9	0.8
ΔNb	–0.71	–0.60	–0.63	–0.64	–1.88	–1.80	–1.30	–1.95	–2.27	–1.54	–1.97	–1.14

Sample name	P98-66	P98-72	P98-59	P98-62	P98-88	P98-95	98DM-151	98DM-158	98DM-162	01MC-013	01MC-116
Rock type	PB	MB	MB	MB	MB	PB	MB	MB	PB	MB	MB
Affinity	E-MORB	E-MORB	E-MORB	E-MORB	E-MORB	E-MORB	E-MORB	E-MORB	E-MORB	BABB	BABB
Al_2O_3/Na_2O	4	4	4	4	4	4	5	7	3	48	243
Al_2O_3/TiO_2	10	10	7	8	10	14	11	11	7	27	13
Ti/V	32	34	39	33	31	29	28	33	36	14	25
Ti/Zr_{pm}	1.00	0.86	0.89	1.00	1.01	1.09	1.30	0.92	1.24	0.64	0.80
Nb/La_{pm}	1.4	1.5	1.5	1.2	1.3	1.3	1.5	1.3	1.3	0.3	0.3
Nb/Th_{pm}	1.7	1.7	1.8	1.6	1.7	1.7	1.9	1.6	1.7	0.3	0.5
Nb/Y	0.22	0.33	0.48	0.43	0.27	0.27	0.27	0.36	0.47	0.04	0.06
Nb/U	44.7	19.4	42.9	30.6	57.9	48.6	53.3	40.8	44.7	5.2	13.6
Nb/Yb	2.5	3.9	5.6	5.0	2.8	3.0	3.1	3.8	5.5	0.4	0.6
Zr/Y	17.3	20.0	20.4	17.0	16.5	14.7	13.2	19.5	15.4	17.6	18.0
Zr/Nb	10.6	9.1	7.3	6.5	9.4	7.8	6.3	8.2	4.9	52.2	41.2
Zr/Yb	26.3	35.2	40.7	32.3	26.2	23.0	19.2	30.8	26.8	22.9	25.4
Hf/Sm	0.58	0.58	0.60	0.57	0.61	0.58	0.53	0.70	0.57	0.73	0.72
La/Sm	1.4	1.6	2.3	2.6	1.8	1.9	1.7	2.2	3.0	1.3	1.7
Sm/Yb	0.7	0.9	1.0	0.9	0.7	0.7	0.6	0.9	0.8	0.7	0.8
ΔNb	–1.29	–1.23	–1.09	–0.99	–1.17	–1.07	–0.98	–1.18	–0.86	–2.02	–1.91

Note: ΔNb = log (Nb/Y) + 1.74 – 1.92 log (Zr/Y) (Fitton et al., 1997). Abbreviations: BABB—backarc basin basalt; DB—diabase; E-MORB—enriched mid-ocean ridge basalt; MB—massive basalt; MG—massive greenstone; N-MORB—normal mid-ocean ridge basalt; OIB—ocean island basalt; PB—pillow basalt; PM—normalized to primitive mantle values of Sun and McDonough (1989); N—north of Jules Creek-Vangorda Fault; S—south of Jules Creek-Vangorda Fault.

TABLE 3. SAMARIUM-NEODYMIUM ISOTOPE GEOCHEMICAL DATA FOR SELECT BASALTIC ROCKS FROM THE CAMPBELL RANGE FORMATION

Sample	Affinity	$^{147}Sm/^{144}Nd$	$^{143}Nd/^{144}Nd$	Uncertainty $\pm 2s_m$	εNd_t	εNd_0	T_{DM}	Sm (ppm)	Nd (ppm)
P98-59B	OIB	0.1226	0.512618	0.000013	2.2	–0.4	0.91	6.28	30.99
P98-77	OIB	0.1209	0.512683	0.000008	3.6	0.9	0.79	6.02	30.14
P98-66	E-MORB	0.1950	0.512941	0.000009	6.0	5.9	–	3.16	9.80
P98-88	E-MORB	0.1881	0.512792	0.000008	3.3	3.0	–	3.30	10.61
P98-95	E-MORB	0.1894	0.512905	0.000010	5.5	5.2	–	2.71	8.66
98DM-162	E-MORB	0.1678	0.512840	0.000010	5.0	3.9	–	4.93	17.76
P98-63	N-MORB (S)	0.2036	0.512964	0.000007	6.1	6.4	–	4.16	12.34
P98-78	N-MORB (S)	0.1925	0.512427	0.000007	–4	–4.1	–	9.02	28.32
P98-87	N-MORB (S)	0.2032	0.513011	0.000016	7.1	7.3	–	3.31	9.86
01MC-007	N-MORB (N)	0.2330	0.513089	0.000007	7.5	8.8	–	2.91	7.54
01MC-114	N-MORB (N)	0.2113	0.513118	0.000006	8.9	9.4	–	3.22	9.22
01MC-013	BABB	0.2084	0.512988	0.000008	6.4	6.8	–	2.09	6.06
01MC-116	BABB	0.1895	0.513066	0.000006	8.6	8.4	–	3.35	10.70

Note: Abbreviations: BABB—backarc basin basalt; E-MORB—enriched mid-ocean ridge basalt; N-MORB—normal mid-ocean ridge basalt; OIB—ocean-island basalt; N—north of Jules Creek-Vangorda Fault; S—south of Jules Creek-Vangorda Fault.

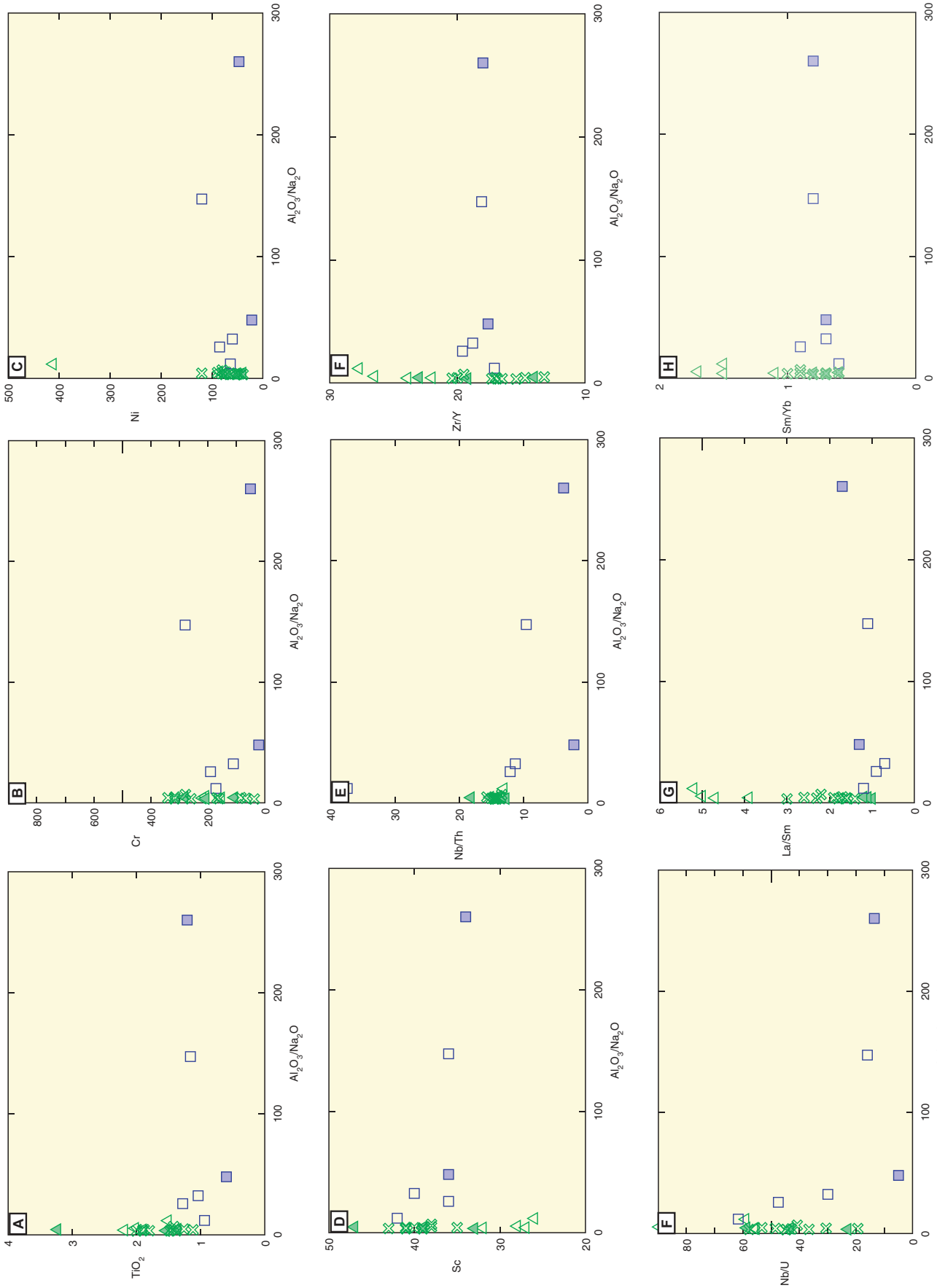

Figure 5. Key trace elements and element ratios against the Spitz-Darling (Spitz and Darling, 1978) Al_2O_3/Na_2O alteration index. The lack of correlation between the various elements and ratios with the alteration index suggests that the variance in these elements is independent of alteration and thus that they were immobile during alteration and metamorphism.

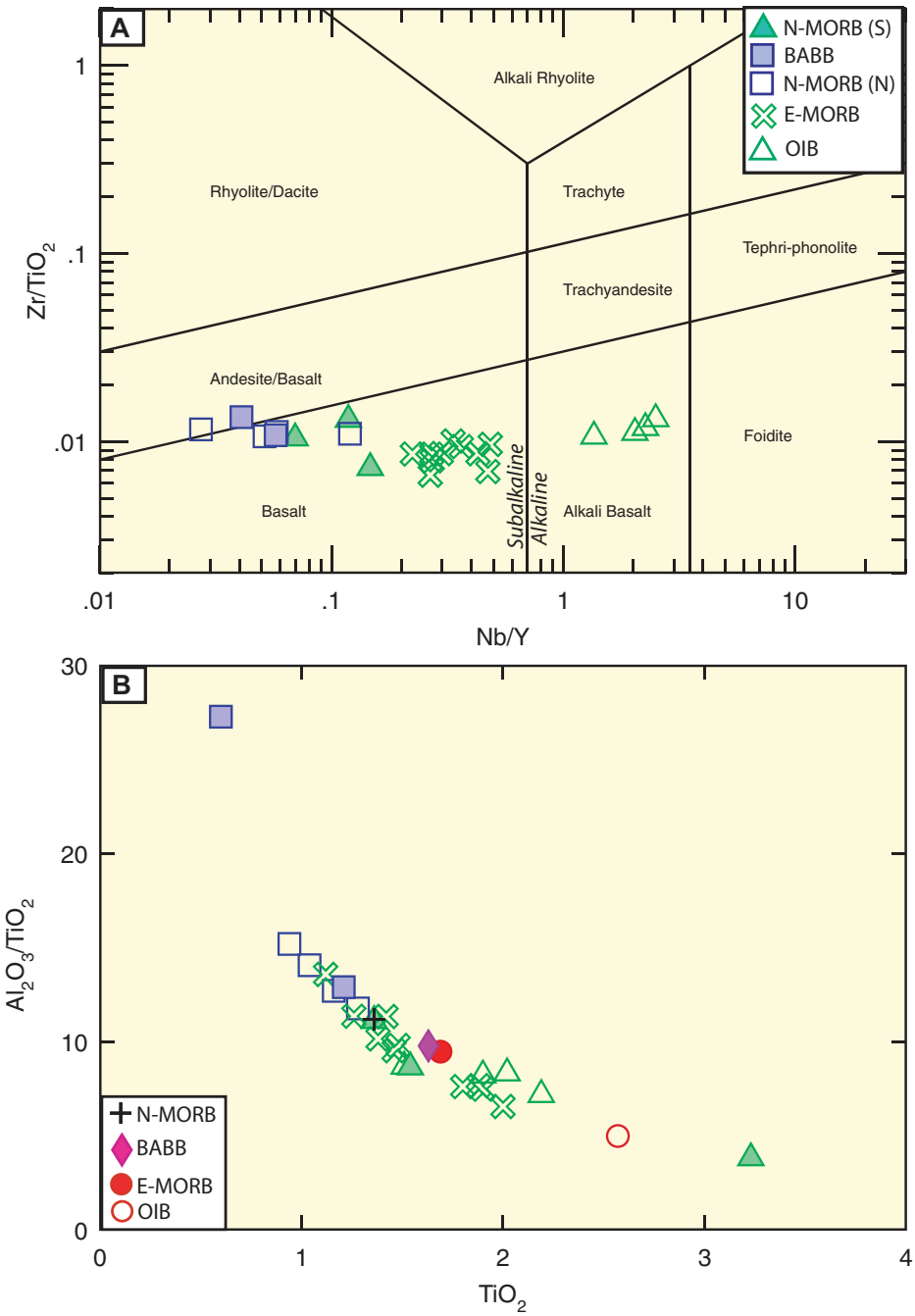

Figure 6. Niobium/Y-Zr/TiO_2 discrimination diagram (A) of Winchester and Floyd (1977) as modified by Pearce (1996); and Al_2O_3/TiO_2-TiO_2 plot (B). Mid-ocean ridge basalt (MORB), enriched mid-ocean ridge basalt (E-MORB), and ocean-island basalt (OIB) data from Sun and McDonough (1989). BABB—backarc basin basalt; N-MORB—normal mid-ocean ridge basalt.

contents than other suites in the Campbell Range Formation (Table 1). The elevated HFSE and REE contents of the basalts are illustrated by their steep primitive mantle–normalized trace element profiles (Fig. 7A), which are characterized by strong light rare-earth element (LREE) enrichment (La/Sm = 3.9–5.2), heavy rare-earth element (HREE) depletion (Sm/Yb = 1.1–1.7), and distinctive positive Nb anomalies relative to Th (Nb/Th_{pm} = 1.6–1.7) and La (Nb/La_{mn} = 1.8–2.0). The OIB suite has distinctive incompatible-element ratios that point to derivation from enriched, OIB-like, mantle sources (Fig. 8). Furthermore, they have lower εNd values compared to other suites in the Campbell Range Formation (Fig. 8; Table 3). In comparison to the other suites in the Campbell Range Formation, they have the lowest Zr/Nb and Hf/Sm ratios and highest Zr/Y, Nb/Y, Zr/Yb, Nb/Yb, Ti/Yb, La/Sm, Sm/Yb, Nb/La_{pm}, and Nb/Th_{pm} values (Figs. 8–10; Table 2); furthermore, they have ΔNb >0, pointing to derivation from an enriched source (Fig. 8; Table 2; Fitton et al., 1997; Baksi, 2001; Condie, 2003). The Ti/V ratios of the OIB-suite rocks are also consistent with the OIB-like attributes of these rocks, and they lie within the field for nonarc, alkalic rocks on the Ti-V plot of Shervais (1982) (Fig. 9).

Isotopically, the OIB suite has the lowest $εNd_t$ values in the Campbell Range Formation with two samples yielding $εNd_t$ = +2.2 and +3.6 (Table 3; Fig. 10). These values are much lower than the depleted mantle (DM) reservoir at 275 Ma, which has $εNd_t$ = +9.5 (Fig. 10), and suggest that the OIB suite has been derived from a source, or has had influence from a reservoir, with a history of LREE enrichment (i.e., Sm/Nd <CHUR; Goldstein et al., 1984; DePaolo, 1988). Furthermore, the OIB suite has sufficiently low Sm/Nd ratios (Sm/Nd <0.3), such that the rocks may have meaningful depleted mantle model ages (T_{DM}), and yields T_{DM} ages of 0.79 Ga and 0.91 Ga (Table 3).

N-MORB Suite

Rocks having N-MORB affinities have basaltic Zr/TiO_2 values and subalkalic Nb/Y values (Nb/Y 0 <0.7; Fig. 6). They have the lowest HFSE and REE concentrations (Table 1) and the lowest TiO_2 contents (TiO_2 = 0.94%–3.23%, avg. = 1.51%) of all the Campbell Range Formation samples, with Al_2O_3/TiO_2 values (Al_2O_3/TiO_2 = 4–15, avg. = 11) akin to modern N-MORB (Al_2O_3/TiO_2 ~11; Fig. 6; Sun and McDonough, 1989). The low HFSE and REE concentrations are illustrated by the smooth but LREE-depleted (La/Sm = 0.7–1.2) primitive mantle–normalized trace element profiles (Figs. 7C and 7D). Furthermore, the N-MORB suite is undepleted in HREE (Sm/Yb = 0.6–0.9), has high Nb relative to Th (Nb/Th_{mn} = 1.2–4.5; Table 2), but low to flat Nb relative to La (Nb/La_{mn} = 0.5–1.3; Table 2; Figs. 7C, 7D, and 8). The N-MORB samples north of the Jules Creek–Vangorda fault (Fig. 7D) have lower overall concentrations of trace elements when compared to those south of the fault (Fig. 7C), despite similar overall patterns. The N-MORB suite lies along the HFSE- and LREE-depleted portion of the Campbell Range εNd array (Fig. 10) and, in contrast to the OIB suite, is consistent with derivation from an incompatible-element–depleted mantle source region. The depleted nature of the N-MORB suite is echoed by their high Zr/Nb and Hf/Sm ratios, lowest

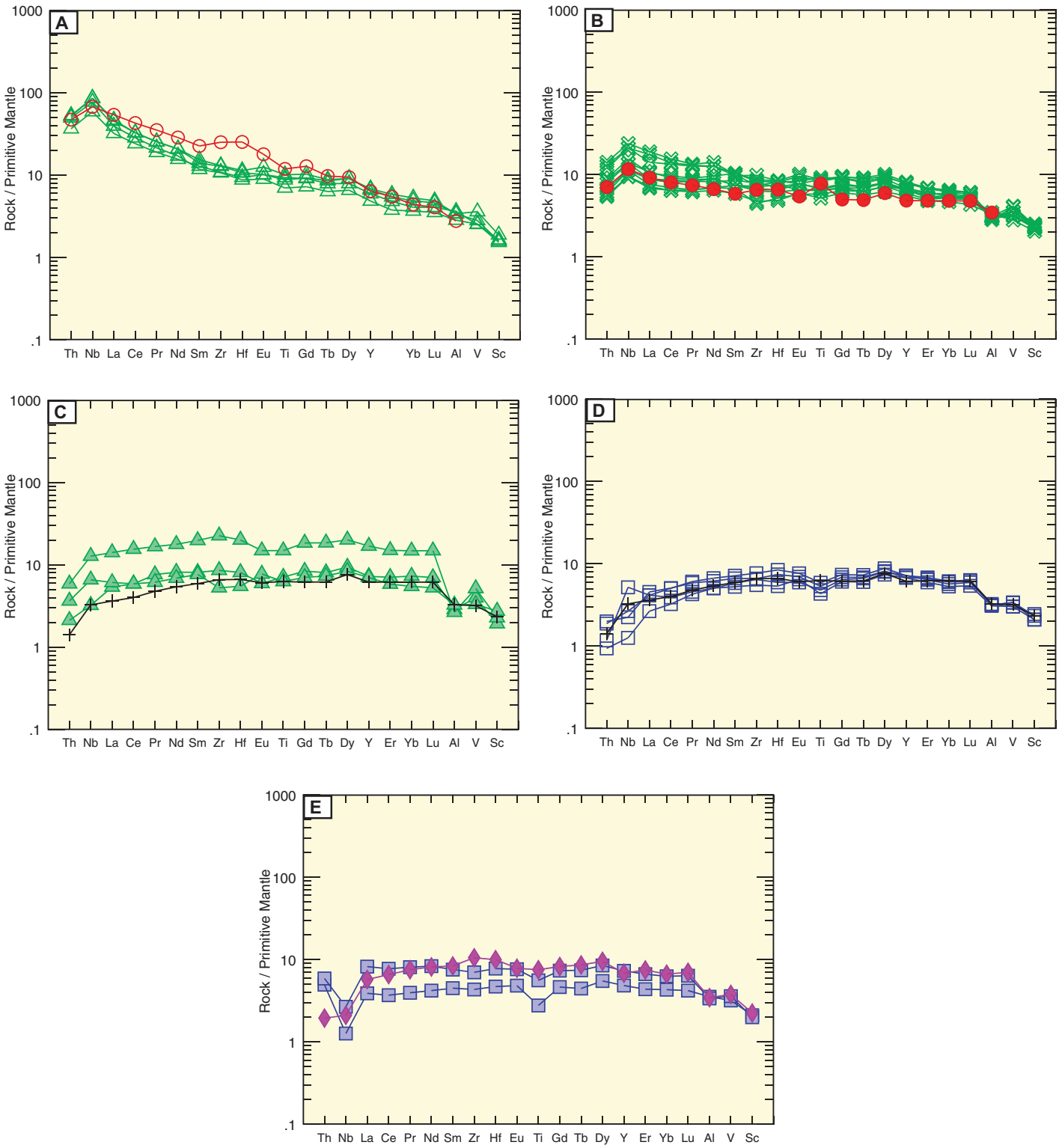

Figure 7. Primitive-mantle–normalized plots of (A) ocean-island basalt (OIB); (B) enriched mid-ocean ridge basalt (E-MORB); (C) normal mid-ocean ridge basalt (N-MORB) south of the Jules Creek fault; (D) N-MORB north of the Jules Creek fault; and (E) backarc basin basalt (BABB) suite rocks with modern analogues on each plot for comparison. Primitive-mantle normalization values from Sun and McDonough (1989). Modern N-MORB, E-MORB, and OIB from Sun and McDonough (1989) and backarc basin basalt (BABB) from Ewart et al. (1994).

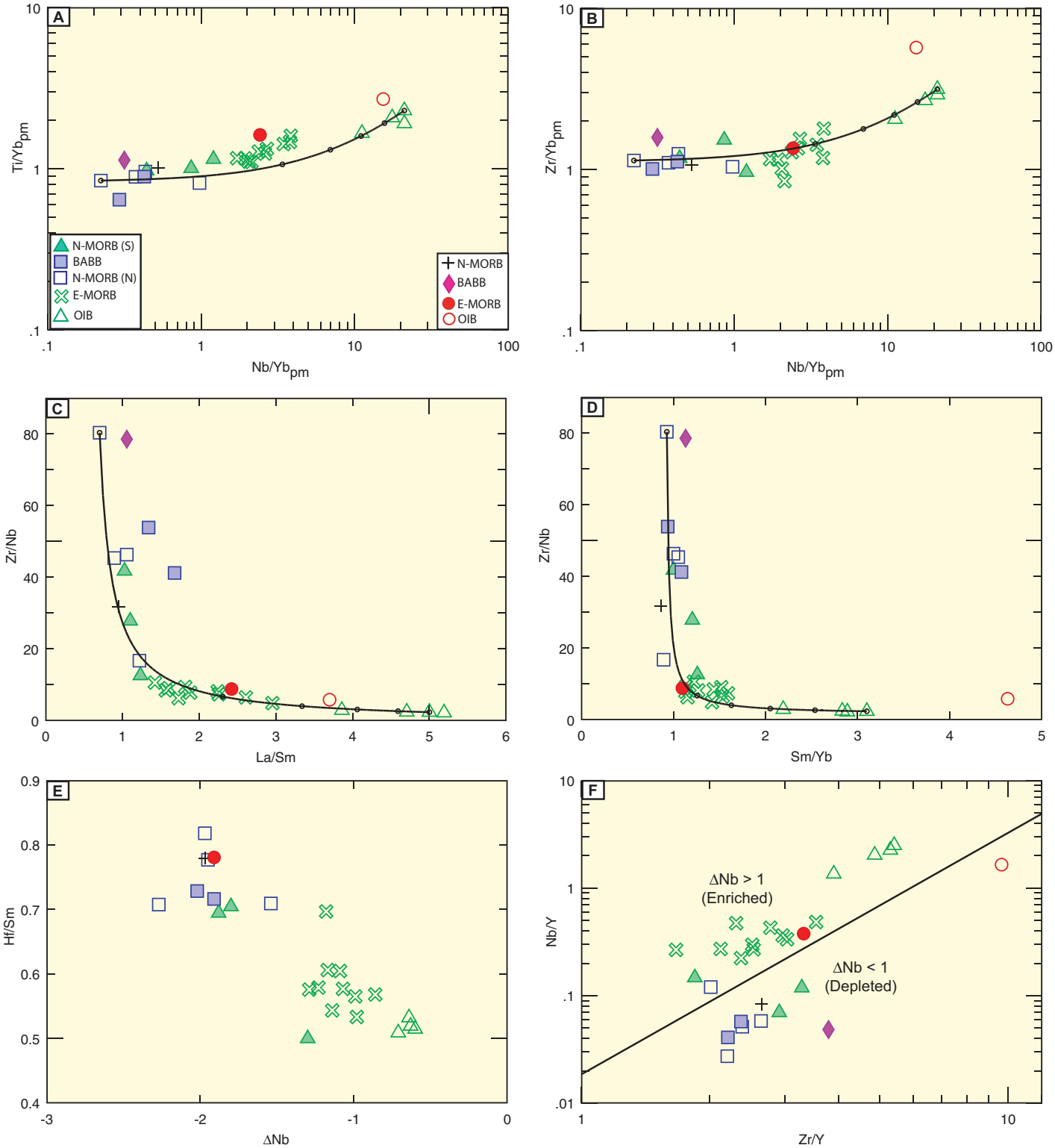

Figure 8. Incompatible trace element plots illustrating that the different suites of the Campbell Range Formation lie on a mixing line with varying contributions from an enriched, ocean-island basalt (OIB)–like end member and a depleted, normal–mid-ocean ridge basalt (N-MORB)–like end member. Diagrams include: (A) Ti/Yb_{pm}-Nb/Yb_{pm} (pm—primitive-mantle normalized) and Zr/Yb_{pm}-Nb/Yb_{pm} (B) (after Pearce and Peate, 1995); (C) Zr/Nb-La/Sm; (D) Zr/Nb-Sm/Yb; (E) Hf/Sm-ΔNb; and (F) Zr/Y-Nb/Y plot. Plot of ΔNb in (F) from Fitton et al. (1997) and Baksi (2001), where ΔNb = 1.74 + 0.92 log(Y/Zr) + log(Nb/Zr). BABB—backarc basin basalt; E-MORB—enriched mid-ocean ridge basalt.

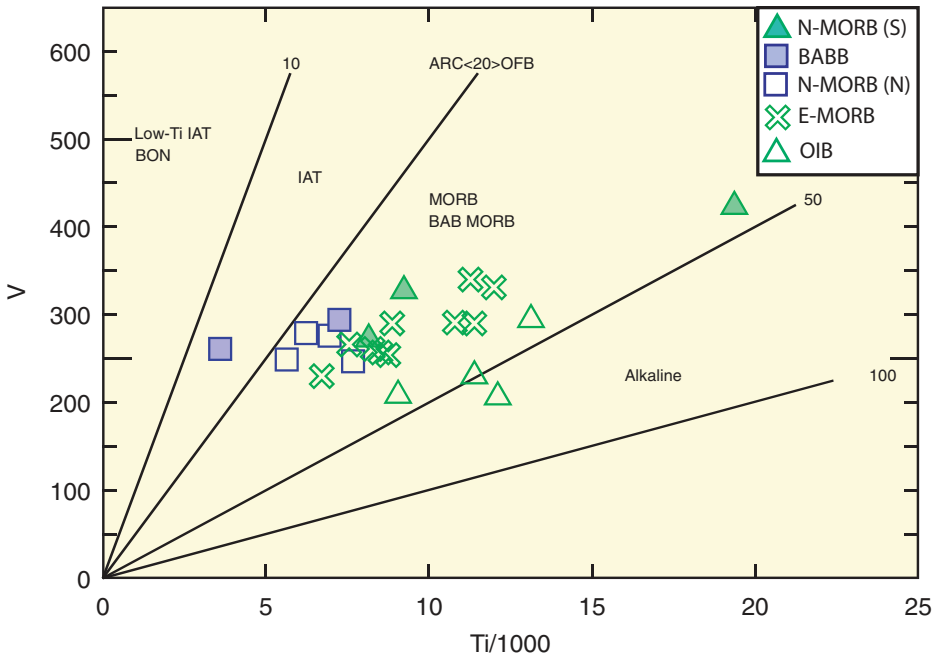

Figure 9. Discrimination diagram of Ti/V from Shervais (1982) illustrating the backarc basinal nature of the rocks from the Campbell Range belt. BABB—backarc basin basalt; E-MORB—enriched mid-ocean ridge basalt; N-MORB—normal mid-ocean ridge basalt; OIB—ocean-island basalt.

Zr/Y, Nb/Y, Zr/Yb, Nb/Yb, Ti/Yb, La/Sm, and Sm/Yb ratios, and Nb/La_{pm} and Nb/Th_{pm} values (Fig. 8; Table 2). Furthermore, they have ΔNb <0, pointing to derivation from a depleted source (Fig. 8; Table 2; Fitton et al., 1997; Baksi, 2001; Condie, 2003). The low Ti/V ratios of the N-MORB suite are consistent with formation within a nonarc (or backarc) geodynamic environment (Fig. 9; Table 2).

The N-MORB suite has the highest average εNd_t values of all basalts in the Campbell Range Formation with most samples ranging from +6.1 to +8.9, with the exception of P98-78, which has εNd_t = –4.0 (Table 3; Fig. 10). There are differences, albeit slight, between the samples north and south of the Jules Creek fault, with samples north of the fault having εNd_t = +7.5 to +8.9, whereas those south of the fault range from εNd_t = –4.0 to +7.1 (Table 3). With the exception of sample P98-78, this range is similar to slightly less than the DM reservoir at this time (εNd_t = +9.5; Goldstein et al., 1984; DePaolo, 1988) and suggests derivation from a reservoir with a history of LREE depletion (i.e., Sm/Nd >CHUR; Goldstein et al., 1984; DePaolo, 1988).

E-MORB Suite

Samples of the E-MORB suite have basaltic affinities with low Zr/TiO_2 and subalkalic Nb/Y values (Nb/Y 0 < 0.7; Fig. 6). The E-MORB suite has TiO_2 contents (1.12%–2.00%, avg. = 1.57%) intermediate between the N-MORB and OIB suite, with Al_2O_3/TiO_2 (7–14, avg. 9.5) ratios very similar to E-MORB (Al_2O_3/TiO_2 = 9.5; Fig. 6) (Sun and McDonough, 1989). The E-MORB suite has primitive mantle–normalized patterns that are intermediate between the N-MORB and OIB suites, with relatively flat to enriched LREE (La/Sm = 1.4–3.0; Table 2), weakly positive Nb anomalies relative to Th (Nb/Th_{mn} = 1.6–1.9; Table 2) and La (Nb/La_{mn} = 1.2–1.5; Table 2), and relatively flat HREE (Sm/Yb = 0.6–1.0; Table 2; Figs. 7 and 8). The E-MORB suite lies in an intermediate position in the Campbell Range Formation array between the OIB and N-MORB end members (Fig. 8). The intermediate position of the E-MORB suite is reflected by incompatible-element ratio values (Zr/Nb, Hf/Sm, Zr/Y, Nb/Y, Zr/Yb, Nb/Yb, Ti/Yb, La/Sm, Sm/Yb, Nb/La_{pm}, and Nb/Th_{pm}) that are intermediate between N-MORB and OIB (Fig. 8; Table 2). Notable, however, is that the E-MORB suite still has ΔNb values >0, suggesting a significant contribution from enriched mantle sources (Fig. 7; Table 2; Fitton et al., 1997; Baksi, 2001; Condie, 2003). Like the N-MORB and OIB suites, the Ti/V ratios of the E-MORB suite imply formation within a nonarc (or backarc) geodynamic environment (Fig. 9; Table 2).

Samples of the E-MORB suite have intermediate εNd_t values with εNd_t = +3.3 to +6.0, which is slightly lower than the DM reservoir at this time (εNd_t = +9.5; Goldstein et al., 1984; DePaolo, 1988), and intermediate between the N-MORB and OIB suites (Table 3; Fig. 10).

BABB Suite

The BABB suite is identical to the N-MORB suite, but with weakly developed negative Nb and Ti anomalies. It exhibits low TiO_2 content (0.6–1.2 wt%) with Al_2O_3/TiO_2 values slightly higher than the N-MORB suite (13–27; Fig. 6; Tables 1 and 2), a feature common to BABB suite rocks (e.g., Woodhead et al., 1993; Stolper and Newman, 1994; Hawkins, 1995; Newman et al., 2000; Taylor and Martinez, 2003). The primitive mantle–normalized trace element patterns of the BABB suite differ from the N-MORB suite by having a distinctive negative Nb anomaly relative to Th and La (Nb/Th_{mn} = 0.3–0.5; Nb/La_{mn} ~0.3; Table 2; Fig. 7). This anomaly is the "subduction signature" present in most modern BABB suites (e.g., Fryer et al., 1990; Hawkins, 1995; Taylor and Martinez, 2003). Akin to the MORB suite, the BABB suite lies toward the depleted end of the Campbell Range Formation array with high Zr/Nb and Hf/Sm ratios, low Zr/Y, Nb/Y, Zr/Yb, Nb/Yb, Ti/Yb, La/Sm, and Sm/Yb ratios, and Nb/La_{pm} and Nb/Th_{pm} values, and ΔNb <0, all pointing to derivation from an depleted mantle source region (Fig. 7; Table 2; Fitton et al., 1997; Baksi, 2001; Condie, 2003). The Ti-V systematics of the BABB suite are similar to that of the N-MORB suite, but the BABB suite straddles the arc-nonarc boundary on the Ti-V plot (Fig. 9), similar to their transitional Th-Nb-La systematics (Fig. 7) and consistent with derivation in a backarc basin geodynamic setting.

The Nd-isotopic signature of the BABB suite is virtually identical to that of the N-MORB suite with εNd_t = +6.4 and +8.6 (Fig. 10; Table 3), implying derivation from a similar depleted mantle source, but with a weak subduction component added to that depleted source (i.e., lower Nb/Th relative to N-MORB; e.g., Fryer et al., 1990; Hawkins, 1995; Taylor and Martinez, 2003).

GEOGRAPHIC DISTRIBUTION OF GEOCHEMICAL SUITES

The different geochemical suites in the Campbell Range Formation show a systematic pattern with respect to the Jules Creek–Vangorda fault, marking the fault as an important lithospheric break and supporting its interpretation as a significant transcurrent fault. North of the fault, where the formation is stratigraphically underlain by basinal clastic rocks and chert of the Fortin Creek group, the rocks are N-MORB

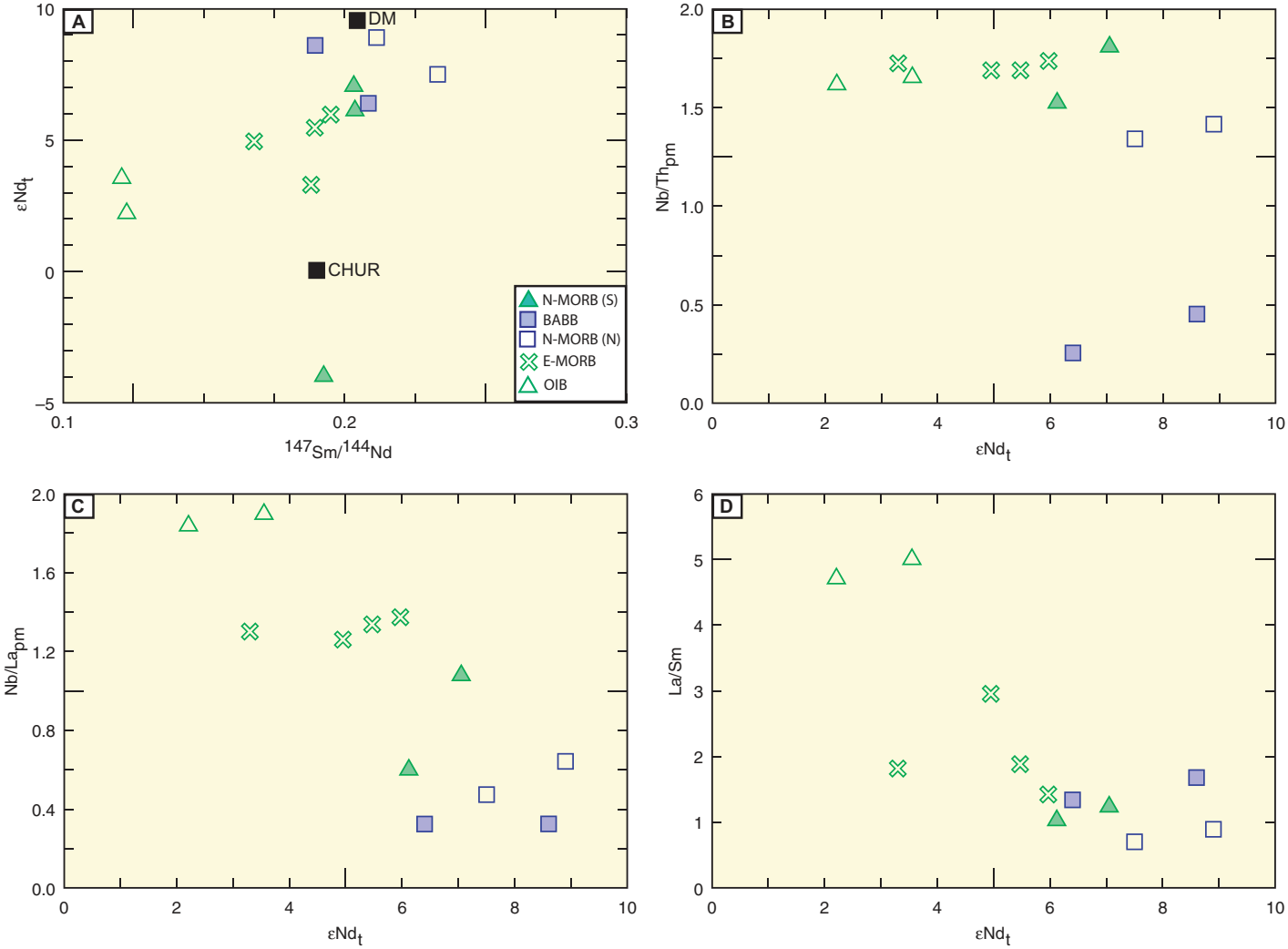

Figure 10. Ratios for εNd_t and $^{147}Sm/^{144}Nd$ progressively decrease from the normal mid-ocean ridge basalt (N-MORB) and backarc basin basalt (BABB) suite, through the enriched mid-ocean ridge basalt (E-MORB) suite, to the ocean-island basalt (OIB) suite (A) reflecting derivation from progressively incompatible-element–enriched mantle. The flat to inverse relationships between εNd_t and Nb/Th_{pm} (B), Nb/La_{pm} (C), and La/Sm (D) illustrate that the lower εNd_t values in the more incompatible-element–enriched samples (i.e., OIB and E-MORB) are features of the source region rather than due to crustal contamination. If crustal contamination were controlling the εNd_t distribution of these rocks, a positive relationship between εNd_t and these variables would be expected.

to BABB in affinity, with no samples having incompatible-element–enriched signatures (i.e., no E-MORB or OIB; Fig. 11). South of the fault, the Campbell Range Formation is stratigraphically underlain by rocks of the ensialic Yukon-Tanana terrane, and E-MORB signatures predominate, with lesser OIB and N-MORB signatures (Fig. 11). Neodymium isotopic signatures also vary systematically across the fault. South of the fault, the rocks have εNd_t = +2.2 to +3.6 for the OIB suite and εNd_t = +3.3 to +6.0 for the E-MORB suite, whereas N-MORBs have values ranging from εNd_t = –4.0 to +7.1 (Table 3; Fig. 11). The N-MORB and BABB suites north of the fault have εNd_t = +7.5 to +8.9 and εNd_t = +6.4 to +8.6, respectively, values that overlap those south of the fault but fall toward higher εNd_t (Fig. 11).

The stratigraphic relationships between the various suites cannot be determined owing to limitations of outcrop exposure and lack of stratigraphic markers. South of the Jules Creek–Vangorda fault, samples of E-MORB, OIB, and N-MORB occur in relatively close proximity, suggesting that these samples are stratigraphically interlayered (Fig. 11). A similar case can be made for the samples north of the fault, as samples of both N-MORB and BABB character are spatially associated with one another, and the BABB could be equivalent to the N-MORB suite but with a greater subduction component (Fig. 11) (Hawkins, 1995; Gribble et al., 1996; Taylor and Martinez, 2003).

One explanation for the contrast in isotopic and geochemical character of the Campbell Range Formation basalts across the Jules Creek–Vangorda fault is that the rocks on opposite sides of the fault formed along the fault in different parts of the backarc basin and were subsequently juxtaposed along it (e.g., Fig. 12). In the next section, we present evidence that the geochemical and isotopic diversity of the Campbell Range basalts is a consequence of mixing of magmas from different source regions and that basalt north of the fault is

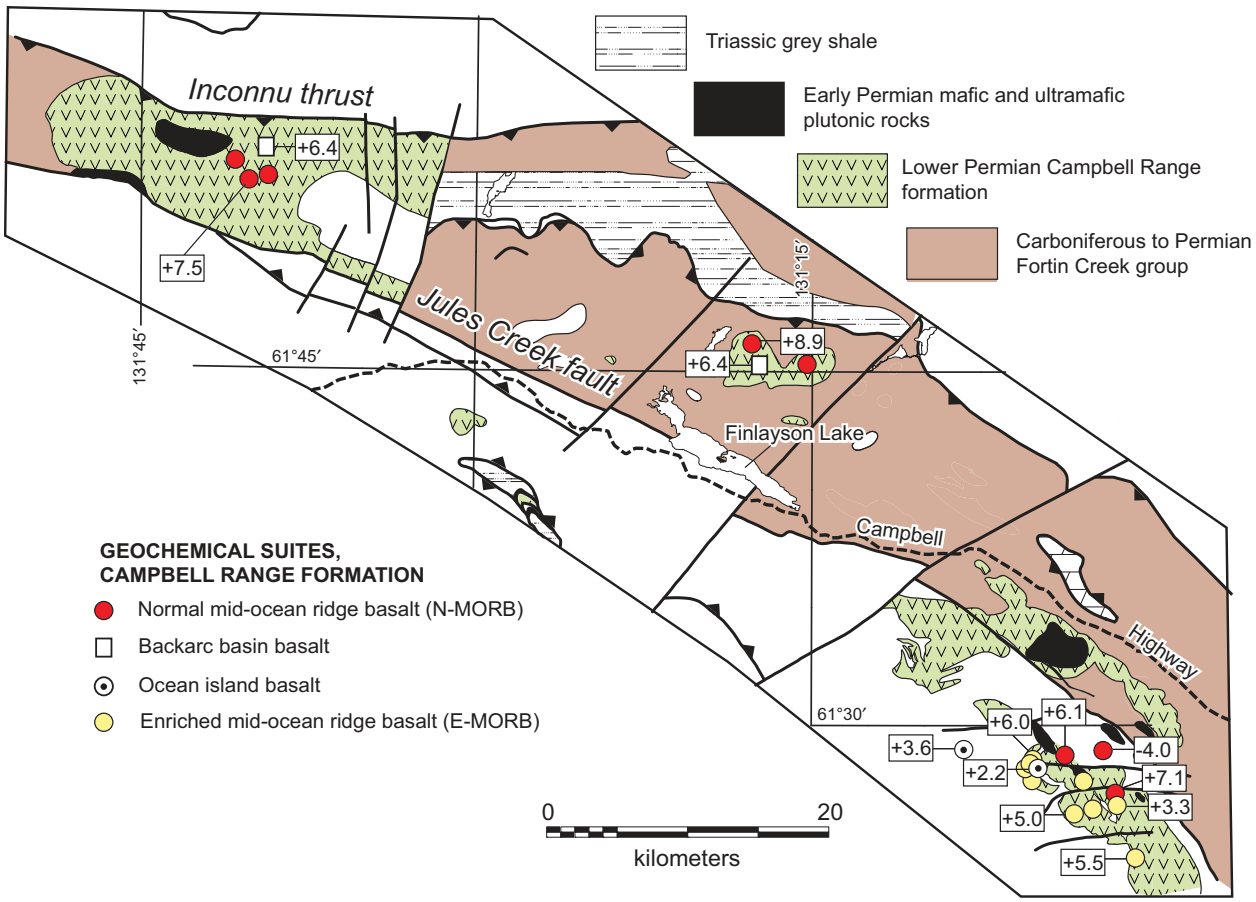

Figure 11. Distribution of different lithogeochemical suites from the Campbell Range Formation and their relationship to the Jules Creek–Vangorda fault. Notably, all rocks with enriched signatures lie south of the Jules Creek fault.

sourced primarily from depleted mantle melts, while basalt south of the fault is sourced from magma derived from melting of depleted and enriched mantle sources.

MAGMA SOURCE CHARACTERISTICS OF THE CAMPBELL RANGE BASALTS

The geochemical and isotopic data for Campbell Range Formation basaltic rocks consistently lie on arrays between N-MORB and OIB end members (Figs. 7, 8, and 10), implying that the various suites formed as variable mixtures of incompatible-element–enriched and –depleted mantle. The BABB suite also formed from N-MORB-like mantle (Fig. 7; e.g., Hawkins, 1995; Gribble et al., 1996), but the suite has higher La/Sm, and lower Nb/La_{mn} due to La and Th addition associated with the introduction of a subducted slab component into this N-MORB mantle (e.g., You et al., 1996; Fig. 7; Tables 1 and 2). The derivation of Campbell Range basalts from mixtures of enriched and depleted mantle is also supported by Nd isotopic data in which there is a progressive shift toward lower εNd_t values, with exceptions being the most incompatible-element–enriched basalts (i.e., E-MORB and OIB, Fig. 10; Table 3). It is also notable that the BABB suite has identical isotopic signatures to the N-MORB suites (εNd_t = +6.8 to +8.4), implying derivation from an isotopically similar source. An important implication of the isotopic differences between the enriched and depleted suites is that isotopically distinct end members are required, ruling out the possibility that their geochemical differences are due to variable degrees of partial melting of a common source region (Fig. 10). Crustal contamination is also improbable because Nb/La_{mn}, Nb/Th_{mn}, and La/Sm (with the exception of the BABB suite) progressively decrease with increasing εNd_t (Fig. 10), the opposite to what would be expected if crustal contamination was the main cause for the variation in εNd_t (i.e., Nb/La_{mn} and Nb/Th_{mn} should decrease, and La/Sm should increase with decreasing εNd_t).

Given the unlikelihood of crustal contamination, mixing of melts from a heterogeneous source area best explains the variation in isotopic and incompatible-element geochemistry for the Campbell Range basaltic rocks. In order to quantify the degree of mixing between different end members, the isotopic mixing equation of Faure (1986) is employed:

$$R_x^m = \left[R_x^1 C_1 X + R_x^2 C_2 (1-X)\right] / \left[C_1 X + C_2 (1-X)\right], \quad (1)$$

where R_x^m = isotopic ratio of the mixture (e.g., εNd_t or $^{143}Nd/^{144}Nd$); R_x^1 and R_x^2 are the isotopic compositions of the end members; C_1 and C_2 are the Nd concentrations of the end members; and X is a proportionality factor that ranges from 0 to 1. In the case where X = 1, then the mixture consists entirely of component C_1; whereas, in the case where X = 0, it consists entirely of C_2; values that are mixtures lie between these two end members. In the isotopic mixing equations, the most depleted and enriched end members have been chosen according to those with the highest and lowest εNd_t values, respectively, from the N-MORB and OIB groups, respectively (Table 3). The results of these calculations are presented in Table 4 and illustrate that the N-MORB and BABB suites have contributions

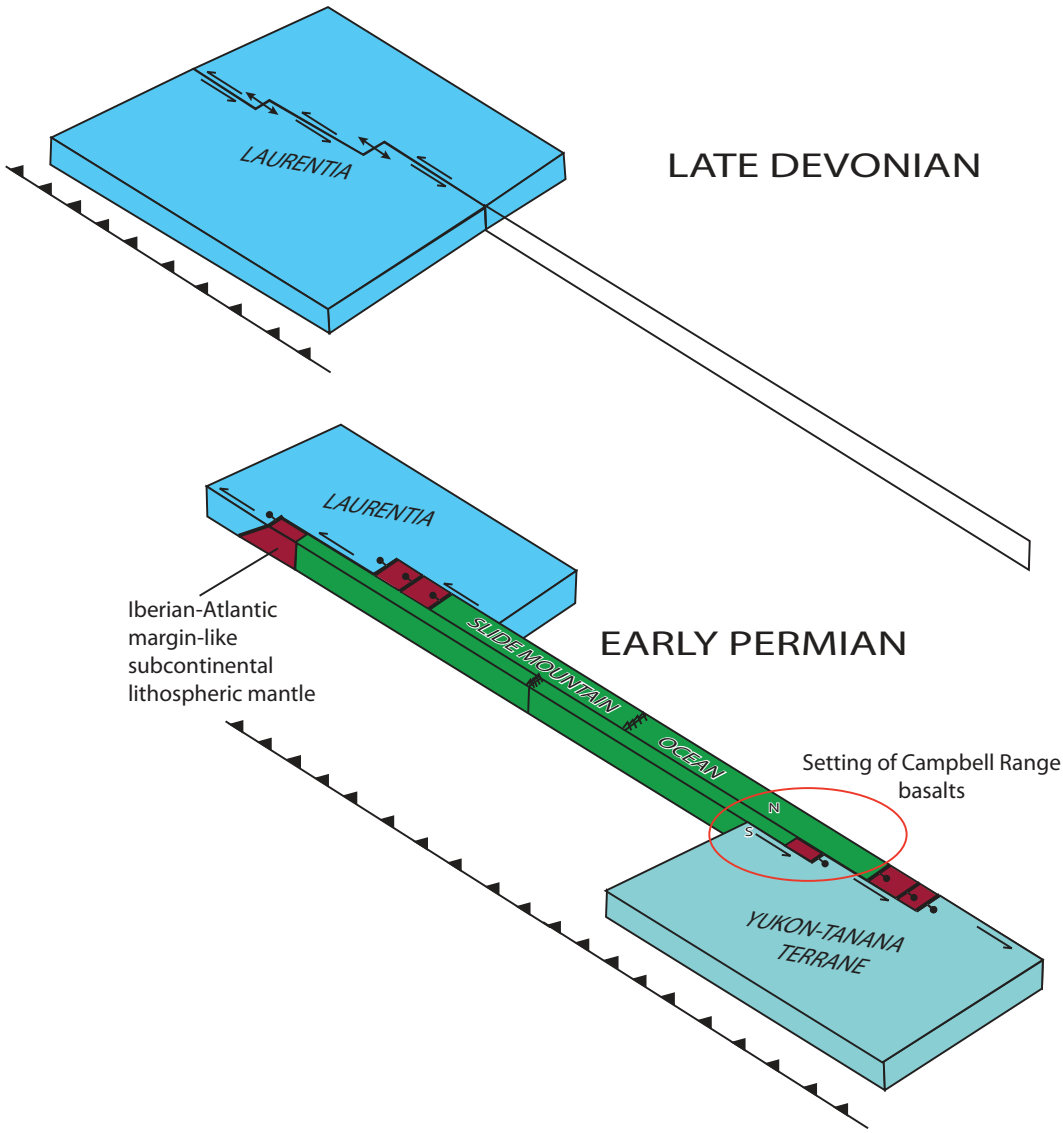

Figure 12. Proposed setting of Early Permian Campbell Range magmatism, along transform faults bounding Yukon-Tanana terrane and different domains within the Slide Mountain ocean. This model is a transform-dominated end member: Carboniferous rifting within the Slide Mountain ocean may have been more orthogonal, creating a wider ocean basin. However, the latitudinal transport implicit in the Permian McCloud fauna of the pericratonic terranes requires significant displacement on sinistral transform faults either within the basin or at its margins.

from enriched sources between 0% and 17%, with an average contribution of 8% (excluding sample P98-78). The OIB end member is dominated by the enriched component (54%–100%); whereas the E-MORB suite is consistent with mixing between the depleted and enriched end members with between 19% and 62%, with an average enriched component value of 33% (Table 4).

To further quantify the amount of mixing between the end members, and to provide a multi-element supplement to the Nd-isotopic data, binary elemental mixing equations for the most highly incompatible elements (Nb, Zr, Hf, Th, La, Ce, Pr, Nd, and Sm) are used. The binary mixing equation is given by the following (Faure, 1986):

$$C_m = C_1X + C_2(1-X), \qquad (2)$$

where C_m = concentration of element i in the mixture (i.e., the sample), C_1 and C_2 are the concentrations of element i in end members 1 and 2, and X is a proportionality factor as described above. As with the incompatible-element plots described previously (e.g., Fig. 8), we have chosen this group of highly incompatible elements because they provide the best insight into the nature of the sources for the basalts (e.g., Pearce and Peate, 1995), and they will provide the best estimates of the degrees of mixing. Furthermore, the middle REE (MREE) to HREE, being more compatible and less sensitive to variations between enriched and depleted end members, were not used in the mixing models. Since mixing between two end members provides a single solution (i.e., a single proportion of the different end members), by having a number of different elements, there are more variables than unknowns, and to solve this type of system, a least-squares solution for the elements outlined above has been obtained (see Appendix A for details of the model and Table 5 for results). Notably, in this model, the choice of end members is slightly different than in the isotopic mixing calculations because there is slight decoupling between the most depleted and enriched samples isotopically and elementally. In selecting the end members, the samples that are most depleted and enriched in HFSE and REE, respectively (P98-77, enriched end member; 01MC-007, depleted end member), have been chosen. The results from the multicomponent model are very similar to those of the model reliant solely on isotopic data (Tables 4 and 5). In particular, the OIB suite contains primarily enriched material ranging from 69% to 100% (average = 87%); the N-MORB

TABLE 4. RESULTS FROM ISOTOPIC MIXING MODEL USING ND-ISOTOPIC DATA

Sample	Affinity	Nd	εNd_t	X
P98-59B*	OIB	30.99	2.2	**1.00**
P98-77	OIB	30.14	3.5	0.54
Average ocean-island basalt				**0.77**
P98-63	N-MORB (S)	12.34	6.1	0.17
P98-78	N-MORB (S)	28.32	–4.0	–1.61
P98-87	N-MORB (S)	9.86	7.1	0.10
01MC-007	N-MORB (N)	7.54	7.5	0.07
01MC-114[1]	N-MORB (N)	9.22	8.9	**0.00**
Average normal mid-ocean ridge basalt				***0.09***
P98-66	E-MORB	9.80	6.0	0.19
P98-88	E-MORB	10.61	3.3	0.60
P98-95	E-MORB	8.66	5.5	0.24
98DM-162	E-MORB	17.76	4.9	0.30
Average enriched mid-ocean ridge basalt				***0.33***
01MC-013	BABB	6.06	6.4	0.15
01MC-116	BABB	10.70	8.6	0.01
Average backarc basin basalt				***0.08***
Average backarc basin basalt + mid-ocean ridge basalt				***0.08***

*end-member compositions.
Note: Abbreviations: BABB—backarc basin basalt; E-MORB—enriched mid-ocean ridge basalt; N-MORB—normal mid-ocean ridge basalt; OIB—ocean-island basalt; N—north of Jules Creek-Vangorda Fault; S—south of Jules Creek-Vangorda Fault.

and BABB are derived from predominantly depleted sources with 0%–21% enriched component (average 6%); whereas the E-MORB suite represents a mixture between the two end members with 10%–30% enriched component (average = 18%) (Table 5). The beauty of the multicomponent mixing model, however, is that it does not rely solely on one isotopic value, provides a solution based on a greater number of variables, and can be calculated on samples that have not had any radiogenic isotopic analysis.

DISCUSSION

Magma Mixing and the Settings of Campbell Range Magmatism

Although our modeling of the geochemical and isotopic data for the Campbell Range Formation indicates that mixing of melts from different mantle sources occurred, the nature of this mixing is not well constrained by physical and chemical attributes. For example, is this mixing between deep mantle plumes or enriched mantle and depleted upper mantle along a spreading ridge or backarc spreading center (e.g., Iceland or New Zealand; Fitton et al., 1997; Huang et al., 2000; Kempton et al., 2000)? Is it due to melting of a "plum pudding" mantle with blobs of enriched eclogitic or garnet-pyroxenitic material within a depleted matrix (e.g., Allègre et al., 1984; Zindler et al., 1984; Niu and Batiza, 1997; Niu et al., 1999)? Or is it due to mixing between enriched subcontinental lithospheric mantle and depleted asthenospheric upper mantle (e.g., Daley and DePaolo, 1992; DePaolo and Daley, 2000)?

A deep mantle plume as the source of enriched material in Slide Mountain rocks has been advocated by Lapierre et al. (2003), and is consistent with the geochemical attributes of these rocks (e.g., Fig. 7; Tables 1 and 2). In nearly all cases, plume magmatism is typically associated with: (1) a high volume of OIB-like magmas and (2) domal uplift and upward shallowing of sedimentary facies (Rainbird, 1993; Rainbird and Ernst, 2001), neither of which is observed in the Campbell Range Formation. Most geological evidence points to thinning of the crust and extensional activity (e.g., synvolcanic faults), rather than crustal thickening; no evidence exists for shallowing of sedimentary facies (Murphy and Piercey, 2000; Murphy et al., 2002). Furthermore, the OIB-like magmas are restricted to the area near the Jules Creek–Vangorda fault and are of minor volume (Fig. 11, Murphy et al., 2006).

Although the Campbell Range Formation may not have formed from a mantle plume, the low HREE and high LREE/HREE ratios in some samples clearly require "garnet" influence during their genesis. Many workers have discussed the "garnet signature" in MORB, suggesting that it may reflect a heterogeneous "plum pudding" mantle made up of enriched garnet-bearing domains, be they eclogite or pyroxenite, within a depleted spinel peridotite matrix (Allègre et al., 1984; Zindler et al., 1984; Allègre and Turcotte, 1986; Zindler and Hart, 1986; Langmuir et al., 1992; Hirschmann and Stolper, 1996; Niu and Batiza, 1997; Niu et al., 1999). A plum-pudding mantle with eclogitic or garnet-pyroxenite veins could account for the geochemical diversity in the Campbell Range Formation. The more enriched garnet-bearing domains could account for the OIB-like

TABLE 5. RESULTS FROM MULTICOMPONENT ELEMENTAL MIXING MODELS

Sample	Affinity	X
P98-77*	OIB	**1.00**
P98-59A	OIB	0.69
P98-59B	OIB	1.01
P98-60	OIB	0.89
Average ocean-island basalt	–	***0.87***
01MC-007*	N-MORB (N)	**0.00**
P98-63	N-MORB (S)	0.04
P98-78	N-MORB (S)	0.21
P98-87	N-MORB (S)	0.07
01CR-113	N-MORB (N)	0.03
01MC-008	N-MORB (N)	0.03
01MC-114	N-MORB (N)	0.03
Average normal mid-ocean ridge basalt	–	***0.07***
P98-61	E-MORB	0.18
P98-66	E-MORB	0.10
P98-72	E-MORB	0.15
P98-59	E-MORB	0.26
P98-62	E-MORB	0.27
P98-88	E-MORB	0.13
P98-95	E-MORB	0.10
98DM-151	E-MORB	0.11
98DM-158	E-MORB	0.16
98DM-162	E-MORB	0.30
Average enriched mid-ocean ridge basalt	–	***0.18***
01MC-013	BABB	0.02
01MC-116	BABB	0.07
Average backarc basin basalt	–	***0.04***
Average backarc basin basalt + mid-ocean ridge basalt	–	***0.06***

*mixing model end members.
Note: Abbreviations: BABB—backarc basin basalt; E-MORB—enriched mid-ocean ridge basalt; N-MORB—normal mid-ocean ridge basalt; N—north of Jules-Creek-Vangorda Fault; S—south of Jules Creek-Vangorda Fault.

signatures, the depleted matrix could account for the N-MORB and BABB signatures, and mixtures of the two could account for the E-MORB signatures (Fig. 8). Similar results have been observed in the East Pacific Rise, where workers have suggested that the enriched plums reside as physically distinct domains in a depleted matrix, and when melted result in melt-induced mixing between the depleted and enriched end members (Niu et al., 1996; Niu and Batiza, 1997; Niu et al., 1999). This type of mantle-melting mechanism could also occur within a mature backarc basin in which oceanic crust is forming.

We favor a variant of the plum-pudding model where the enriched garnet-pyroxenite or eclogitic lithologies reside in the subcontinental lithospheric mantle (e.g., Hawkesworth et al., 1990; McDonough, 1990; Menzies, 1990; Pouclet et al., 1995; DePaolo and Daley, 2000) and interact with upwelling depleted asthenosphere during rifting in the Campbell Range backarc basin. This model involves backarc spreading and transform faulting behind an extending continental arc system (Fig. 12, e.g., Piercey et al., 2006). In this model, the dominant enriched component resides in the subcontinental lithospheric mantle along a continent-bordering transform fault—magmatism would be in large part derived from the OIB-like lithospheric sources. With continued spreading and upwelling, coupled with the juxtaposition of oceanic and continental lithosphere along transform faults, depleted N-MORB asthenosphere interacts and mixes with lithospheric mantle leading to the formation of the E-MORB suite. With full-fledged seafloor spreading and extension, asthenospheric mantle dominates in the melting regime. In this model, the BABB suite is derived from an N-MORB–type asthenospheric source with minor influence from subducted slab metasomatism (e.g., Fryer et al., 1990; Hawkins, 1995; Pouclet et al., 1995). A similar model of asthenosphere-lithosphere evolution has been proposed to account for the observed shift from more alkalic to MORB-like basalts with time during the Miocene to Holocene evolution of Sea of Japan (Fig. 12) (Pouclet et al., 1995).

Implications for the Geodynamic Evolution of Slide Mountain Terrane

Geological and paleontological data suggest that the Slide Mountain backarc basin was transform-dominated both during its opening and closing. Such a basin would have numerous settings where the two different geochemical and isotopic domains of the Campbell Range could form and be juxtaposed (Figs. 11 and 12). The domain sourced in depleted mantle lithosphere north of the fault (Fig. 11) could form along any one of the numerous intra-oceanic rift segments. In contrast, the domain with both depleted and enriched melt sources would lie only along the transforms bordering the ensialic Yukon-Tanana lithosphere (Fig. 12). Because these structures link directly to spreading centers, the juxtaposition of these two settings would naturally occur with increasing amounts of displacement. Hence, our model of the formation and juxtaposition of the two different domains along transform faults is entirely consistent with the transform-dominated nature of the Slide Mountain ocean (Fig. 12).

The Jules Creek–Vangorda fault system is the manifestation of the transform nature of this backarc basin and likely represents a leaky sinistral transform fault that separated the Yukon-Tanana ensialic arc terrane from its coeval obliquely opening backarc basin recorded by the Campbell Range Formation. The occurrence of Campbell Range Formation basalt and, importantly, affiliated plutonic rocks that occur on both sides of the Jules Creek–Vangorda fault for over a 300 km strike length, but only within a few kilometers of it, suggests that the fault is the first-order control on the emplacement of intrusions and volcanism. Because the Campbell Range Formation occurs at about the same elevation on both sides of the fault, normal- or thrust-sense displacement can be ruled out, leaving strike-slip as the only alternative. The presence of Middle Permian McCloud fauna in Yukon-Tanana terrane (Ross, 1969; Miller, 1987; Stevens, 1995) also suggests that in the Early Permian the terrane must have been traveling to more southerly latitudes relative to Laurentia. This motion must have been accommodated by sinistral transcurrent structures in or behind the coeval Devono-Carboniferous arc rocks represented by the ~281 Ma Klinkit Group and correlative rocks of the Yukon-Tanana terrane (Simard et al., 2003; Roots et al., 2006). We infer that the Jules Creek–Vangorda fault is one of these structures.

Both regional and local considerations suggest that the Jules Creek–Vangorda fault may have been reactivated as a dextral fault in the Late Permian and again in the Mesozoic. Between the Middle Permian, when characteristic Yukon-Tanana terrane was at the latitude of Texas, and the Middle Triassic, when Yukon-Tanana terrane detrital zircons first appear in rocks of the northwestern North American continental margin sequence (Beranek, 2009; Beranek et al., 2010), the Slide Mountain ocean must have closed and Yukon-Tanana terrane translated dextrally by at least the same amount as it was translated sinistrally during the opening of the Slide Mountain ocean. Some of this displacement may have been partitioned onto the Jules Creek–Vangorda fault. Mesozoic reactivation is indicated by the observation that near Faro, the Campbell Range Formation is juxtaposed along the fault against Upper Triassic to Lower Jurassic (Beranek, 2009) conglomerate and Permian eclogite (Erdmer et al., 1998; Pigage, 2004).

Implications for Crustal Growth at the Western North American Continental Margin

The growth of continental crust reflect the balance between the addition of juvenile material from the mantle versus the recycling of previously formed evolved crust (Patchett and Arndt, 1986; Samson et al., 1989; Condie, 1990, 1998, 2000; Samson and Patchett, 1991; Patchett, 1992; McCulloch and Bennett, 1994; Hawkesworth and Kemp, 2006; Hawkesworth et al., 2010; Condie et al., 2011). During Earth's history, many of the major crustal growth periods (e.g., Neoarchean, Paleoproterozoic, and Neoproterozoic) have been associated with major mantle plume events and/or accretionary tectonic activity, whereby significant masses of juvenile crust have been added either via magmatism or accretion to the crust (e.g., Patchett and Arndt, 1986; McCulloch and Samson et al., 1989; Condie, 1990; Samson and Patchett, 1991; Patchett, 1992; Bennett, 1994; Condie, 1998, 2000; Hawkesworth and Kemp, 2006; Hawkesworth et al., 2010). The evolution of convergent continental margin environments is marked by significant crustal recycling via weathering (e.g., Creaser et al., 1997; Piercey and Colpron, 2009) and the incorporation of crust into felsic magmatic rocks via assimilation (e.g., Hildreth and Moorbath, 1988). Juvenile crustal growth along these continental margins has largely been attributed to trapping of juvenile crust during accretion rather than through magmatism (Condie et al., 2011).

Numerous studies that have pointed out the importance of recycling of crust along the mid to late Paleozoic convergent western margin of Laurentia (Mortensen, 1992b; Creaser et al., 1997; Garzione et al., 1997; Gehrels and Ross, 1998; Patchett and Gehrels, 1998; Mortensen et al., 2006; Piercey et al., 2006; Piercey and Colpron, 2009); however, the importance of juvenile crustal additions to the orogen has not been fully evaluated (Creaser et al., 1997; Patchett and Gehrels, 1998; Creaser et al., 1999; Simard et al., 2003; Piercey et al., 2004). It is notable that during the Pennsylvanian to Early Permian there was extensive juvenile magmatism, both in Yukon-Tanana and in the coeval Slide Mountain backarc ocean, with juvenile isotopic signatures (i.e., $\varepsilon Nd_t > 0$) recorded in both the Yukon-Tanana terrane (Simard et al., 2003)

and in the Slide Mountain terrane (Klepacki, 1985; Struik and Orchard, 1985; Nelson, 1993; Roback et al., 1994; Ferri, 1997; Lapierre et al., 2003; this study). Despite episodic rifting over a 100-million-year history within the Slide Mountain ocean starting in the Late Devonian, igneous rocks of Pennsylvanian to Early Permian age are disproportionately preserved, and those that are preserved have predominantly juvenile isotopic signatures.

The Devonian to Permian backarc opening and closing of the Slide Mountain ocean along the western margin of the North American continent resulted in the accretion of the Slide Mountain terrane onto the cratonic margin (e.g., Nelson et al., 2006), suggesting that the Slide Mountain terrane potentially added significant juvenile crust to the continents and represents net juvenile crustal growth. However, despite their juvenile signatures, the Slide Mountain terrane represents relatively thin structural flakes atop a predominantly continental substrate (e.g., Nelson, 1993); therefore, they likely only represent minor contributors to Cordilleran juvenile crustal growth.

SUMMARY AND CONCLUSIONS

The Lower Permian Campbell Range Formation in the Finlayson Lake region of Yukon is part of the Slide Mountain terrane, a North American Cordilleran–long backarc basinal assemblage that developed between an ensialic arc system and the North American craton in the middle to late Paleozoic. It contains abundant basaltic and high-level intrusive rocks with trace element geochemical signatures similar to modern backarc basin assemblages, including ocean-island basalt (OIB), enriched mid-ocean ridge basalt (E-MORB), normal mid-ocean ridge basalt (N-NORB), and backarc basin basalts (BABB). The range of signatures is mirrored by their Nd isotopic characteristics, which range from εNd_t = +2.2 to +8.9. The geochemical and isotopic diversity is attributed to derivation from mantle sources that range from incompatible-element–enriched (e.g., OIB) through incompatible-element–depleted mantle (e.g., MORB and BABB). The εNd_t values show an inverse relationship with Nb/Th_{pm} and Nb/La_{pm}, suggesting that the lower εNd_t values are a feature of the source of the basalts and not due to continental crustal contamination. We interpret the geochemical and isotopic characteristics of the Campbell Range Formation in the context of a model of an extending continental-backarc basin in which there are varying contributions from the lithospheric and asthenospheric mantle; their formation and juxtaposition is attributed to magmatism along a leaky transform fault within the basin. Isotopic and multielement mixing calculations illustrate that the OIB-like suite was derived primarily from enriched continental lithospheric mantle, whereas the N-MORB and BABB suites were sourced primarily from the upwelling backarc asthenospheric mantle; E-MORB represent mixtures of depleted asthenospheric and enriched lithospheric mantle.

The presence of OIB and E-MORB suites in the Campbell Range Formation and elsewhere in Slide Mountain terrane has been previously attributed to mantle plume magmatism within this backarc basin. The geological features of the OIB and E-MORB suites are inconsistent with a plume origin; however, we infer that they represent OIB-type material derived from the melting of lithospheric mantle during backarc basin formation. The occurrence of juvenile magmatism in the Campbell Range Formation illustrates that backarc basins, like the Slide Mountain ocean, may have contributed to Cordilleran juvenile crustal growth. However, the Slide Mountain terrane, including the Campbell Range Formation, form very thin crustal slivers atop a predominantly continental crustal substrate. Therefore, their net contribution to Cordilleran juvenile crustal growth was minimal.

ACKNOWLEDGMENTS

This study was supported by the Yukon Geological Survey, Geological Survey of Canada Ancient Pacific Margin National Mapping (NATMAP) project, and a Natural Sciences and Engineering Research Council of Canada (NSERC) Discovery Grant to Piercey. Piercey is also funded by the NSERC-Altius Research Chair in Mineral Deposits at Memorial University, which is supported by financial contributions from the NSERC, Altius Resources, Inc., and the Industrial Research Innovation Fund (IRIF) from the Research and Development Corporation of Newfoundland and Labrador. The Radiogenic Isotope Facility at the University of Alberta is supported by a Major Resources Support Grant from NSERC. Discussions with our colleagues in the Ancient Pacific Margin NATMAP project are gratefully acknowledged with special thanks to JoAnne Nelson and Maurice Colpron for ongoing dialogue. Kelly Russell is thanked for insight into matrix models for the mixing equations presented in this paper. Maurice Colpron is thanked for a review of an earlier draft of this manuscript. We thank JoAnne Nelson, an anonymous reviewer, and *Geosphere* Associate Editor Terry Pavlis for formal reviews; their contributions have greatly improved the manuscript.

APPENDIX A: DETAILS OF MULTI-ELEMENT MIXING MODELS

The mixing equation:

$$C_m = C_1X + C_2(1-X) \quad (3)$$

employed in the elemental mixing calculations can be rearranged as follows:

$$(C_1 - C_2)X = (C_m - C_2), \quad (4)$$

which results in a series of linear equations for the different elements with a common proportionality factor (X). In the mixing model, we have used elements that are sensitive to source variations, namely the moderate to highly incompatible elements: Nb, Zr, Hf, Th, La, Ce, Pr, Nd, and Sm. Using the above elements results in a series of linear equations of the form:

$$\begin{aligned}
(Nb_1 - Nb_2)X &= (Nb_m - Nb_2)\\
(Zr_1 - Zr_2)X &= (Zr_m - Zr_2)\\
(Hf_1 - Hf_2)X &= (Hf_m - Hf_2)\\
\ldots\ldots\ldots\ldots &= \ldots\ldots\ldots\ldots\\
(Sm_1 - Sm_2)X &= (Sm_m - Sm_2).
\end{aligned}$$

This series of equations can be written in matrix form as follows, and is a matrix of the form AX = B:

$$\begin{bmatrix} Nb_1 - Nb_2 \\ Zr_1 - Zr_2 \\ Hf_1 - Hf_2 \\ \ldots\ldots\ldots\ldots \\ \ldots\ldots\ldots\ldots \\ Sm_1 - Sm_2 \end{bmatrix} X = \begin{bmatrix} Nb_m - Nb_2 \\ Zr_m - Zr_2 \\ Hf_m - Hf_2 \\ \ldots\ldots\ldots\ldots \\ \ldots\ldots\ldots\ldots \\ Sm_m - Sm_2 \end{bmatrix}.$$

Because this is an over-determined system of equations, it requires solving in the least-squares sense and obtaining the optimum estimate for X:

$$X = \begin{bmatrix} Nb_1 - Nb_2 \\ Zr_1 - Zr_2 \\ Hf_1 - Hf_2 \\ \ldots\ldots\ldots\ldots \\ \ldots\ldots\ldots\ldots \\ Sm_1 - Sm_2 \end{bmatrix}^{-1} \begin{bmatrix} Nb_m - Nb_2 \\ Zr_m - Zr_2 \\ Hf_m - Hf_2 \\ \ldots\ldots\ldots\ldots \\ \ldots\ldots\ldots\ldots \\ Sm_m - Sm_2 \end{bmatrix}.$$

This mixing model provides the best estimate of mixing, takes into account all input elements, and returns the optimum solution for the model (e.g., Albarade, 1996; Davis, 2002).

REFERENCES CITED

Albarade, F., 1996, Introduction to Geochemical Modeling: Cambridge, UK, Cambridge University Press, 543 p.

Allègre, C.J., and Turcotte, D.L., 1986, Implications of a two-component marble cake mantle: Nature, v. 323, p. 123–127, doi:10.1038/323123a0.

Allègre, C.J., Hamelin, B., and Dupré, B., 1984, Statistical analysis of isotopic ratios in MORB: The mantle blob cluster model and the convective regime of the mantle: Earth and Planetary Science Letters, v. 71, p. 71–84, doi:10.1016/0012-821X(84)90053-0.

Baksi, A.K., 2001, Search for a deep-mantle component in mafic lavas using a Nb-Y-Zr plot: Canadian Journal of Earth Sciences, v. 38, no. 5, p. 813–824.

Belasky, P., Stevens, C.H., and Hanger, R.A., 2002, Early Permian location of western North American terranes based on brachiopod, fusulinid, and coral biogeography: Palaeogeography, Palaeoclimatology, Palaeoecology, v. 179, p. 245–266, doi:10.1016/S0031-0182(01)00437-0.

Beranek, L.P., 2009, Provenance and paleotectonic setting of North American Triassic strata in Yukon: The sedimentary record of pericratonic terrane accretion in the northern Canadian Cordillera [Ph.D. thesis]: Vancouver, University of British Columbia, 324 p.

Beranek, L.P., Mortensen, J.K., Orchard, M.J., and Ullrich, T., 2010, Provenance of North American Triassic strata from west-central and southeastern Yukon: Correlations with coeval strata in the Western Canada

Sedimentary Basin and Canadian Arctic Islands: Canadian Journal of Earth Sciences, v. 47, no. 1, p. 53–73, doi:10.1139/E09-065.

Burnham, O.M., and Schweyer, J., 2004, Trace element analysis of geological samples by inductively coupled plasma mass spectrometry at the geoscience laboratories: Revised capabilities due to improvements to instrumentation: Summary of fieldwork and other activities 2004: Ontario Geological Survey, p. 54.1–54.20.

Burnham, O.M., Hechler, J., Semenyna, L., and Schweyer, J., 2002, Mineralogical controls on the determination of trace elements following mixed-acid dissolution: Sudbury, Ontario, Ontario Geological Survey Open-File Report 6160, p. 36.1–36.12.

Colpron, M., and Nelson, J.L., 2009, A Palaeozoic Northwest Passage: Incursion of Caledonian, Baltican, and Siberian terranes into eastern Panthalassa, and the early evolution of the North American Cordillera: The Geological Society of London Special Publications, v. 318, no. 1, p. 273–307, doi:10.1144/SP318.10.

Colpron, M., and Nelson, J.L., 2011, Chapter 31: A Paleozoic NW Passage and the Timanian, Caledonian, and Uralian connections of some exotic terranes in the North American Cordillera: The Geological Society of London Memoir 35, no. 1, p. 463–484.

Colpron, M., Nelson, J.L., and Murphy, D.C., 2006, A tectonostratigraphic framework for the pericratonic terranes of the northern Canadian Cordillera, *in* Colpron, M., and Nelson, J.L., eds., Paleozoic Evolution and Metallogeny of Pericratonic Terranes at the Ancient Pacific Margin of North America, Canadian and Alaskan Cordillera: St. John's, Newfoundland and Labrador, Canada, Geological Association of Canada, p. 1–23.

Colpron, M., Nelson, J.L., and Murphy, D.C., 2007, Northern Cordilleran terranes and their interactions through time: GSA Today, v. 17, no. 4, p. 4–10, doi:10.1130/GSAT01704-5A.1.

Condie, K.C., 1990, Growth and accretion of continental crust: Inferences based on Laurentia: Chemical Geology, v. 83, p. 183–194, doi:10.1016/0009-2541(90)90279-G.

Condie, K.C., 1998, Episodic continental growth and supercontinents: A mantle avalanche connection?: Earth and Planetary Science Letters, v. 163, p. 97–108, doi:10.1016/S0012-821X(98)00178-2.

Condie, K.C., 2000, Episodic continental growth models: afterthoughts and extensions: Tectonophysics, v. 322, p. 153–162, doi:10.1016/S0040-1951(00)00061-5.

Condie, K.C., 2003, Incompatible element ratios in oceanic basalts and komatiites: Tracking deep mantle sources and continental growth rates with time: Geochemistry, Geophysics, Geosystems, v. 4, Paper #2002GC000333.

Condie, K.C., Bickford, M.E., Aster, R.C., Belousova, E., and Scholl, D.W., 2011, Episodic zircon ages, Hf isotopic composition, and the preservation rate of continental crust: Geological Society of America Bulletin, v. 123, no. 5–6, p. 951–957, doi:10.1130/B30344.1.

Creaser, R.A., Erdmer, P., Stevens, R.A., and Grant, S.L., 1997, Tectonic affinity of Nisutlin and Anvil assemblage strata from the Teslin tectonic zone, northern Canadian Cordillera: Constraints from neodymium isotope and geochemical evidence: Tectonics, v. 16, p. 107–121, doi:10.1029/96TC03317.

Creaser, R.A., Goodwin-Bell, J.-A.S., and Erdmer, P., 1999, Geochemical and Nd isotopic constraints for the origin of eclogite protoliths, northern Cordillera: Implications for the Paleozoic tectonic evolution of the Yukon-Tanana terrane: Canadian Journal of Earth Sciences, v. 36, no. 10, p. 1697–1709, doi:10.1139/cjes-36-10-1697.

Daley, E.E., and DePaolo, D.J., 1992, Isotopic evidence for lithospheric thinning during extension: Southeastern Great Basin: Geology, v. 20, no. 2, p. 104–108, doi:10.1130/0091-7613(1992)020<0104:IEFLTD>2.3.CO;2.

Davis, J.C., 2002, Statistics and Data Analysis in Geology, Third Edition: New York, John Wiley and Sons, 638 p.

DePaolo, D.J., 1988, Neodymium Isotope Geochemistry: An Introduction: Springer-Verlag, 187 p.

DePaolo, D.J., and Daley, E.E., 2000, Neodymium isotopes in basalts of the Southwest Basin and Range and lithospheric thinning during continental extension: Chemical Geology, v. 169, no. 1–2, p. 157–185, doi:10.1016/S0009-2541(00)00261-8.

Dusel-Bacon, C., and Cooper, K., 1999, Trace-element geochemistry of metabasaltic rocks from the Yukon-Tanana Upland and implications for the origin of tectonic assemblages in east-central Alaska: Canadian Journal of Earth Sciences, v. 36, no. 10, p. 1671–1695, doi:10.1139/cjes-36-10-1671.

Dusel-Bacon, C., Mortensen, J.K., Werdon, M., Newberry, R., Szumigala, D., Day, W., Dashevsky, J., Wooden, J.L., and Aleinikoff, J.N., 2006, Paleozoic tectonic and metallogenic evolution of the Yukon-Tanana terrane, east-central Alaska, *in* Colpron, M., and Nelson, J.L., eds., Paleozoic Evolution and Metallogeny of Pericratonic Terranes at the Ancient Pacific Margin of North America, Canadian and Alaskan Cordillera: St. John's, Newfoundland and Labrador, Canada, Geological Association of Canada, p. 25–74.

Erdmer, P., Ghent, E.D., Archibald, D.A., and Stout, M.Z., 1998, Paleozoic and Mesozoic high-pressure metamorphism at the margin of ancestral North America in central Yukon: Geological Society of America Bulletin, v. 110, p. 615–629, doi:10.1130/0016-7606(1998)110<0615:PAMHPM>2.3.CO;2.

Ewart, A., Bryan, W.B., Chappell, B.W., and Rudnick, R.L., 1994, Regional geochemistry of the Lau-Tonga arc and backarc systems: Proceedings of the Ocean Drilling Program, Scientific Results, May, v. 135, p. 385–425.

Faure, G., 1986, Principles of Isotope Geology, Second Edition: John Wiley and Sons, 608 p.

Ferri, F., 1997, Nina Creek Group and Lay Range Assemblage, north-central British Columbia: Remnants of late Paleozoic oceanic and arc terranes: Canadian Journal of Earth Sciences, v. 34, p. 854–874, doi:10.1139/e17-070.

Fitton, J.G., Saunders, A.D., Norry, M.J., Harwood, D.S., and Taylor, R.N., 1997, Thermal and chemical structure of the Iceland Plume: Earth and Planetary Science Letters, v. 153, no. 3–4, p. 197–208, doi:10.1016/S0012-821X(97)00170-2.

Fryer, P., Taylor, B., Langmuir, C.H., and Hochstaedter, A.G., 1990, Petrology and geochemistry of lavas from the Sumisu and Torishima backarc rifts: Earth and Planetary Science Letters, v. 100, p. 161–178, doi:10.1016/0012-821X(90)90183-X.

Garzione, C.N., Patchett, P.J., Ross, G.M., and Nelson, J., 1997, Provenance of Paleozoic sedimentary rocks in the Canadian Cordilleran miogeocline: A Nd isotopic study: Canadian Journal of Earth Sciences, v. 34, no. 12, p. 1603–1618, doi:10.1139/e17-129.

Gehrels, G.E., and Ross, G.M., 1998, Detrital zircon geochronology of Neoproterozoic to Permian miogeoclinal strata in British Columbia and Alberta: Canadian Journal of Earth Sciences, v. 35, no. 12, p. 1380–1401, doi:10.1139/e98-071.

Goldstein, S.L., O'Nions, R.K., and Hamilton, P.J., 1984, A Sm-Nd isotopic study of atmospheric dusts and particulates from major river systems: Earth and Planetary Science Letters, v. 70, p. 221–236, doi:10.1016/0012-821X(84)90007-4.

Gribble, R.F., Stern, R.J., Bloomer, S.H., Stüben, D., O'Hearn, T., and Newman, S., 1996, MORB mantle and subduction components interact to generate basalts in the Mariana Trough backarc basin: Geochimica et Cosmochimica Acta, v. 60, p. 2153–2166, doi:10.1016/0016-7037(96)00078-6.

Hamilton, P.J., O'Nions, R.K., Bridgwater, D., and Nutman, A., 1983, Sm-Nd studies of Archaean metasediments and metavolcanics from West Greenland and their implications for the Earth's early history: Earth and Planetary Science Letters, v. 62, p. 263–272, doi:10.1016/0012-821X(83)90089-4.

Hawkesworth, C.J., and Kemp, A.I.S., 2006, Evolution of the continental crust: Nature, v. 443, p. 811–817, doi:10.1038/nature05191.

Hawkesworth, C.J., Kempton, P.D., Rogers, N.W., Ellam, R.M., and van Calsteren, P.W., 1990, Continental mantle lithosphere, and shallow level enrichment processes in the Earth's mantle: Earth and Planetary Science Letters, v. 96, p. 256–268, doi:10.1016/0012-821X(90)90006-J.

Hawkesworth, C.J., Dhuime, B., Pietranik, A.B., Cawood, P.A., Kemp, A.I.S., and Storey, C.D., 2010, The generation and evolution of the continental crust: Journal of the Geological Society of London, v. 167, no. 2, p. 229–248, doi:10.1144/0016-76492009-072.

Hawkins, J.W., 1995, Evolution of the Lau Basin - Insights from ODP Leg 135, *in* Taylor, B., and Natland, J., eds., Active Margins and Marginal Basins of the Western Pacific: American Geophysical Union Geophysical Monograph, American Geophysical Union, p. 125–173.

Hildreth, W., and Moorbath, S., 1988, Crustal contribution to arc magmatism in the Andes of Central Chile: Contributions to Mineralogy and Petrology, v. 98, p. 455–489, doi:10.1007/BF00372365.

Hirschmann, M.M., and Stolper, E.M., 1996, A possible role for garnet pyroxenite in the origin of the "garnet signature" in MORB: Contributions to Mineralogy and Petrology, v. 124, p. 185–208, doi:10.1007/s004100050184.

Huang, Y., Hawkesworth, C., Smith, I., Van Calsteren, P., and Black, P., 2000, Geochemistry of late Cenozoic basaltic volcanism in Northland and Coromandel, New Zealand: Implications for mantle enrichment processes: Chemical Geology, v. 164, p. 219–238, doi:10.1016/S0009-2541(99)00145-X.

Jenner, G.A., 1996, Trace element geochemistry of igneous rocks: Geochemical nomenclature and analytical geochemistry, *in* Wyman, D.A., ed., Trace Element Geochemistry of Volcanic Rocks: Applications for Massive Sulfide Exploration, Geological Association of Canada, p. 51–77.

Kempton, P.D., Fitton, J.G., Saunders, A.D., Nowell, G.N., Taylor, R.N., Hardarson, B.S., and Pearson, G., 2000, The Iceland Plume in space and time: A Sr-Nd-Pb-Hf study of the North Atlantic rifted margin: Earth and Planetary Science Letters, v. 177, no. 3–4, p. 255–271, doi:10.1016/S0012-821X(00)00047-9.

Klepacki, D.W., 1985, Stratigraphy and structural geology of the Goat Range area, southeastern British Columbia [Ph.D. thesis]: Massachusetts Institute of Technology, 252 p.

Langmuir, C.H., Klein, E.M., and Plank, T., 1992, Petrological systematics of mid-ocean ridge basalts: Constraints on melt generation beneath ocean ridges, *in* Morgan, J.P., Blackman, D.K., and Sinton, J.M., eds., Mantle Flow and Melt Generation at Mid-Ocean Ridges: American Geophysical Union Monograph Series, American Geophysical Union, p. 183–280.

Lapierre, H., Bosch, D., Tardy, M., and Struik, L.C., 2003, Late Paleozoic and Triassic plume-derived magmas in the Canadian Cordillera played a key role in continental crust growth: Chemical Geology, v. 201, p. 55–89, doi:10.1016/S0009-2541(03)00224-9.

Lesher, C.M., Gibson, H.L., and Campbell, I.H., 1986, Composition-volume changes during hydrothermal alteration of andesite at Buttercup Hill, Noranda District, Quebec: Geochimica et Cosmochimica Acta, v. 50, p. 2693–2705, doi:10.1016/0016-7037(86)90219-X.

Lightfoot, P.C., and Farrow, C.E.G., 2002, Geology, geochemistry, and mineralogy of the Worthington offset dike: A genetic model for offset dike mineralization in the Sudbury Igneous Complex: Economic Geology and the Bulletin of the Society of Economic Geologists, v. 97, p. 1419–1446.

MacLean, W.H., 1990, Mass change calculations in altered rock series: Mineralium Deposita, v. 25, p. 44–49.

Mann, R.K., and Mortensen, J.K., 2000, Geology, geochemistry, and lead isotopic analysis of mineralization of the Strike property, Campbell Range, southeastern Yukon, *in* Emond, D.S., and Weston, L.H., eds., Yukon Geology and Exploration 1999: Yukon, Exploration and Geological Services Division, Indian and Northern Affairs Canada, p. 237–245.

Mata, J., Kerrich, R., MacRae, N.D., and Wu, T.-W., 1998, Elemental and isotopic (Sr, Nd, and Pb) characteristics of Madeira Island basalts: Evidence for a composite HIMU-EM I plume fertilizing lithosphere: Canadian Journal of Earth Sciences, v. 35, p. 980–997, doi:10.1139/e98-046.

McCulloch, M.T., and Bennett, V.C., 1994, Progressive growth of the Earth's continental crust and depleted mantle: Geochemical constraints: Geochimica et Cosmochimica Acta, v. 58, no. 21, p. 4717–4738, doi:10.1016/0016-7037(94)90203-8.

McDonough, W.F., 1990, Constraints on the composition of the continental lithospheric mantle: Earth and Planetary Science Letters, v. 101, no. 1, p. 1–18, doi:10.1016/0012-821X(90)90119-I.

Menzies, M.A., 1990, Petrology and geochemistry of the continental mantle; an historical perspective, *in* Menzies, M.A., ed., Continental Mantle: Oxford Monographs on Geology and Geophysics, p. 31–54.

Miller, M.M., 1987, Displaced remnants of a northeast Pacific fringing arc: Upper Paleozoic terranes of Permian McCloud faunal affinity, western U.S: Tectonics, v. 6, p. 807–830, doi:10.1029/TC006i006p00807.

Miller, M.M., 1998, Displaced remnants of a northeast Pacific fringing arc: Upper Paleozoic terranes of Permian McCloud faunal affinity: Western U.S. Tectonics, v. 6, p. 807–830.

Monger, J.W.H., 1997, Plate tectonics and Northern Cordilleran geology: An unfinished revolution: Geoscience Canada, v. 24, no. 4, p. 189–198.

Monger, J.W.H., and Nokleberg, W.J., 1996, Evolution of the northern North American Cordillera: Generation, fragmentation, displacement, and accretion of successive North American plate margin arcs, *in* Coyner, A.R., and Fahey, P.L., eds., Geology and Ore Deposits of the American Cordillera: Reno and Sparks, Nevada, USA, Geological Society of Nevada Symposium Proceedings, p. 1133–1152.

Mortensen, J.K., 1992a, New U-Pb ages for the Slide Mountain Terrane in southeastern Yukon Territory: Radiogenic Age and Isotopic Studies: Report 5, Geological Survey of Canada, p. 167–173.

Mortensen, J.K., 1992b, Pre-Mid-Mesozoic tectonic evolution of the Yukon-Tanana terrane, Yukon and Alaska: Tectonics, v. 11, p. 836–853, doi:10.1029/91TC01169.

Mortensen, J.K., Dusel-Bacon, C., Hunt, J.A., and Gabites, J., 2006, Lead isotopic constraints on the metallogeny of middle and late Paleozoic syngenetic base metal occurrences in the Yukon-Tanana and Slide Mountain–Seventymile terranes and adjacent portions of the North American miogeocline, *in* Colpron, M., and Nelson, J.L., eds., Paleozoic Evolution and Metallogeny of Pericratonic Terranes at the Ancient Pacific Margin of North America, Canadian and Alaskan Cordillera: St. John's, Newfoundland, Geological Association of Canada, p. 261–279.

Murphy, D.C., and Piercey, S.J., 1999, Finlayson Project: Geological evolution of Yukon-Tanana terrane and its relationship to Campbell Range belt, northern Wolverine Lake map area, southeastern Yukon, Yukon Exploration and Geology 1998: Exploration and Geological Services Division, Yukon, Indian, and Northern Affairs Canada, p. 47–62.

Murphy, D.C., and Piercey, S.J., 2000, Syn-mineralization faults and their re-activation, Finlayson Lake massive sulphide district, Yukon-Tanana Terrane, southeastern Yukon, *in* Emond, D.S., and Weston, L.H., eds., Yukon Exploration and Geology 1999, Exploration and Geological Services Division, Yukon, Indian and Northern Affairs Canada, p. 55–66.

Murphy, D.C., Colpron, M., Roots, C.F., Gordey, S.P., and Abbott, J.G., 2002, Finayson Lake Targeted Geoscience Initiative (southeastern Yukon), Part 1: Bedrock geology, *in* Emond, D.S., Weston, L.H., and Lewis, L.L., eds., Yukon Exploration and Geology 2001: Exploration and Geological Services Division, Indian and Northern Affairs Canada, p. 189–207.

Murphy, D.C., Mortensen, J.K., Piercey, S.J., Orchard, M.J., and Gehrels, G.E., 2006, Tectonostratigraphic evolution of Yukon-Tanana terrane, Finlayson Lake massive sulphide district, southeastern Yukon, *in* Colpron, M., and Nelson, J.L., eds., Paleozoic Evolution of Pericratonic Terranes at the Ancient Pacific Margin of North America, Canadian and Alaskan Cordillera: St. John's, Newfoundland and Labrador, Geological Association of Canada, p. 75–105.

Nelson, J.L., 1993, The Sylvester allochthon: Upper Paleozoic marginal-basin and island-arc terranes in northern British Columbia: Canadian Journal of Earth Sciences, v. 30, p. 631–643, doi:10.1139/e93-048.

Nelson, J.L., Colpron, M., Piercey, S.J., Murphy, D.C., Dusel-Bacon, C., and Roots, C.F., 2006, Paleozoic tectonic and metallogenetic evolution of pericratonic terranes in Yukon, northern British Columbia and eastern Alaska, *in* Colpron, M., and Nelson, J.L., eds., Paleozoic Evolution and Metallogeny of Pericratonic Terranes at the Ancient Pacific Margin of North America, Canadian and Alaskan Cordillera: St. John's, Newfoundland and Labrador, Geological Association of Canada, p. 323–360.

Newman, S., Stolper, E., and Stern, R., 2000, H_2O and CO_2 in magmas from the Mariana arc and back arc systems: Geochemistry, Geophysics, Geosystems, v. 1, Paper 1999GC000027.

Niu, Y., and Batiza, R., 1997, Trace element evidence from seamounts for recycled oceanic crust in the Eastern Pacific mantle: Earth and Planetary Science Letters, v. 148, p. 471–483, doi:10.1016/S0012-821X(97)00048-4.

Niu, Y., Waggoner, D.G., Sinton, J.M., and Mahoney, J.J., 1996, Mantle source heterogeneity and melting processes beneath seafloor spreading centers: The East Pacific Rise, 18°–19° S: Journal of Geophysical Research, v. 101, no. 12, p. 27,711–27,733, doi:10.1029/96JB01923.

Niu, Y., Collerson, K.D., Batiza, R., Wendt, J.I., and Regelous, M., 1999, Origin of enriched-type mid-ocean ridge basalt far from mantle plumes: The East Pacific Rise at 11°20′N: Journal of Geophysical Research, v. 104, no. B4, p. 7067–7087, doi:10.1029/1998JB900037.

Patchett, P.J., 1992, Isotopic studies of Proterozoic crustal growth and evolution, *in* Condie, K.C., ed., Proterozoic Crustal Evolution: Developments in Precambrian Geology 10: Amsterdam, Elsevier, p. 481–508.

Patchett, P.J., and Arndt, N.T., 1986, Nd isotopes and tectonics of 1.9–1.7 Ga crustal genesis: Earth and Planetary Science Letters, v. 78, p. 329–338, doi:10.1016/0012-821X(86)90001-4.

Patchett, P.J., and Gehrels, G.E., 1998, Continental influence of Canadian Cordilleran terranes from Nd isotopic study, and significance for crustal growth processes: The Journal of Geology, v. 106, no. 3, p. 269–280, doi:10.1086/516021.

Pearce, J.A., 1996, A user's guide to basalt discrimination diagrams, *in* Wyman, D.A., ed., Trace Element Geochemistry of Volcanic Rocks: Applications for Massive Sulphide Exploration: Geological Association of Canada, v.12, p. 79–113.

Pearce, J.A., and Peate, D.W., 1995, Tectonic implications of the composition of volcanic arc magmas: Annual Review of Earth and Planetary Sciences, v. 23, p. 251–285, doi:10.1146/annurev.ea.23.050195.001343.

Piercey, S.J., and Colpron, M., 2009, Composition and provenance of the Snowcap assemblage, basement to the Yukon-Tanana terrane, northern Cordillera: Implications for Cordilleran crustal growth: Geosphere, v. 5, no. 5, p. 439–464.

Piercey, S.J., Mortensen, J.K., and Creaser, R.A., 2003, Neodymium isotope geochemistry of felsic volcanic and intrusive rocks from the Yukon-Tanana terrane in the Finlayson Lake region, Yukon, Canada: Canadian Journal of Earth Sciences, v. 40, p. 77–97, doi:10.1139/e02-094.

Piercey, S.J., Murphy, D.C., Mortensen, J.K., and Creaser, R.A., 2004, Mid-Paleozoic initiation of the northern Cordilleran marginal backarc basin: Geological, geochemical and neodymium isotopic evidence from the oldest mafic magmatic rocks in Yukon-Tanana terrane, Finlayson Lake district, southeast Yukon, Canada: Geological Society of America Bulletin, v. 116, p. 1087–1106, doi:10.1130/B25162.1.

Piercey, S.J., Nelson, J.L., Colpron, M., Dusel-Bacon, C., Simard, R.-L., and Roots, C.F., 2006, Paleozoic magmatism and crustal recycling along the ancient Pacific margin of North America, northern Cordillera, *in* Colpron, M., and Nelson, J.L., eds., Paleozoic Evolution and Metallogeny of Pericratonic Terranes at the Ancient Pacific Margin of North America, Canadian and Alaskan Cordillera: St. John's, Newfoundland and Labrador, Geological Association of Canada, v. 45, p. 281–322.

Pigage, L.C., 2004, Bedrock geology compilation of the Anvil District (parts of NTS 105K/2, 3, 5, 6, 7 and 11), central Yukon: Yukon Geological Survey, Bulletin 15, 103 p.

Plint, H.E., and Gordon, T.M., 1997, The Slide Mountain terrane and the structural evolution of the Finlayson Lake fault zone, southeastern Yukon: Canadian Journal of Earth Sciences, v. 34, p. 105–126, doi:10.1139/e17-009.

Pouclet, A., Lee, J.-S., Vidal, P., Cousens, B.L., and Bellon, H., 1995, Cretaceous to Cenozoic volcanism in South Korea and in the Sea of Japan: Magmatic constraints on the opening of the backarc basin, *in* Smellie, J.L., ed., Volcanism Associated with Extension at Consuming Plate Margins: The Geological Society of London Special Publication 81, p. 169–181.

Rainbird, R.H., 1993, The sedimentary record of mantle plume uplift preceding eruption of the Neoproterozoic Natkusiak flood basalt: The Journal of Geology, v. 101, no. 3, p. 305–318, doi:10.1086/648225.

Rainbird, R.H., and Ernst, R.E., 2001, The sedimentary record of mantle-plume uplift, *in* Ernst, R.E., and Buchan, K.L., eds., Mantle Plumes: Their Identification through Time: Boulder, Colorado, Geological Society of America Special Paper 352, p. 227–245.

Roback, R.C., Sevigny, J.H., and Walker, N.W., 1994, Tectonic setting of the Slide Mountain terrane, southern British Columbia: Tectonics, v. 13, p. 1242–1258, doi:10.1029/94TC01032.

Roots, C.F., Nelson, J.L, Simard, R.-L., and Harms, T., 2006, Continental fragments, mid-Paleozoic arcs and overlapping late Paleozoic arc and Triassic sedimentation in the Yukon-Tanana terrane of northern British Columbia and southern Yukon, *in* Colpron, M., and Nelson, J.L., eds, Paleozoic Evolution and Metallogeny of Pericratonic Terraces at the Ancient Pacific Margin of North America, Canadian and Alaskan Cordillera: Geological Association of Canada Special Paper, v. 45, p. 153–177.

Ross, C.A., 1969, Upper Paleozoic Fusulinacea Eowaeringella and Wedekindellina from Yukon Territory and Giant Parafusulina from British Columbia: Ottawa, Ontario, Canada, Contributions to Canadian Paleontology, Geological Survey of Canada Bulletin 182.

Samson, S.D., and Patchett, P.J., 1991, The Canadian Cordillera as a modern analogue of Proterozoic crustal growth: Australian Journal of Earth Sciences, v. 38, p. 595–611, doi:10.1080/08120099108727994.

Samson, S.D., McClelland, W.C., Patchett, P.J., Gehrels, G.E., and Anderson, R.G., 1989, Evidence from neodymium isotopes for mantle contributions to Phanerozoic crustal genesis in the Canadian Cordillera: Nature, v. 337, no. 6209, p. 705–709, doi:10.1038/337705a0.

Shervais, J.W., 1982, Ti-V plots and the petrogenesis of modern and ophiolitic lavas: Earth and Planetary Science Letters, v. 59, p. 101–118, doi:10.1016/0012-821X(82)90120-0.

Shinjo, R., 1999, Geochemistry of high Mg andesites and the tectonic evolution of the Okinawa Trough-Ryukyu arc system: Chemical Geology, v. 157, p. 69–88, doi:10.1016/S0009-2541(98)00199-5.

Simard, R.-L., Dostal, J., and Roots, C.F., 2003, Development of Late Paleozoic arcs in the Canadian Cordillera: An example from the Klinkit Group, northern British Columbia and southern Yukon: Canadian Journal of Earth Sciences, v. 40, p. 907–924, doi:10.1139/e03-025.

Smith, A.D., and Lambert, R.S., 1995, Nd, Sr, and Pb isotopic evidence for contrasting origins of late Paleozoic volcanic rocks from the Slide Mountain and Cache Creek terranes, south-central British Columbia: Canadian Journal of Earth Sciences, v. 32, p. 447–459, doi:10.1139/e95-038.

Spitz, G., and Darling, R., 1978, Major and minor element lithogeochemical anomalies surrounding the Louvem copper deposit, Val d'Or, Quebec: Canadian Journal of Earth Sciences, v. 15, p. 1161–1169, doi:10.1139/e78-122.

Stevens, C.H., 1995, A giant parafusulina from east-central Alaska with comparisons to all giant parafusulinids in western North America: Journal of Paleontology, v. 69, p. 802–812.

Stolper, E., and Newman, S., 1994, The role of water in the petrogenesis of Mariana Trough magmas: Earth and Planetary Science Letters, v. 121, no. 3–4, p. 293–325, doi:10.1016/0012-821X(94)90074-4.

Struik, L.C., and Orchard, M.J., 1985, Late Paleozoic conodonts from ribbon chert delineate imbricate thrusts within the Antler Formation of Slide Mountain terrane, central British Columbia: Geology, v. 13, p. 794–798, doi:10.1130/0091-7613(1985)13<794:LPCFRC>2.0.CO;2.

Sun, S.-s., and McDonough, W.F., 1989, Chemical and isotopic systematics of oceanic basalts: Implications for mantle composition and processes, *in* Saunders, A.D., and Norry, M.J., eds., Magmatism in the Ocean Basins, p. 313–345.

Tanaka, T., Togashi, S., Kamioka, H., Amakawa, H., Kagami, H., Hamamoto, T., Yuhara, M., Orihashi, Y., Shigekazu, Y., Shimuzu, H., Kunimaru, T., Takahashi, K., Yanagi, T., Nakano, T., Fujimaki, H., Shinjo, R., Asahara, Y., Tanimizu, M., and Dragusanu, C., 2000, JNdi-1: A neodymium isotopic reference in consistency with LaJolla neodymium: Chemical Geology, v. 168, p. 279–281, doi:10.1016/S0009-2541(00)00198-4.

Taylor, B., and Martinez, F., 2003, Backarc basin basalt systematics: Earth and Planetary Science Letters, v. 210, no. 3–4, p. 481–497, doi:10.1016/S0012-821X(03)00167-5.

Unterschutz, J.L.E., Creaser, R.A., Erdmer, P., Thompson, R.I., and Daughtry, K.L., 2002, North American margin origin of Quesnel Terrane strata in the southern Canadian Cordillera: Inferences from geochemical and Nd isotopic characteristics of Triassic metasedimentary rocks: Geological Society of America Bulletin, v. 114, p. 462–475, doi:10.1130/0016-7606(2002)114<0462:NAMOOQ>2.0.CO;2.

van Staal, C.R., 2007, Pre-Carboniferous tectonic evolution and metallogeny of the Canadian Appalachians, *in* Goodfellow, W.D., ed., Mineral Deposits of Canada: A Synthesis of Major Deposit Types, District Metallogeny, the Evolution of Geological Provinces, and Exploration Methods: Special Publication 5, Mineral Deposits Division, Geological Association of Canada, p. 793–818.

Whitford, D.J., McPherson, W.P.A., and Wallace, D.B., 1989, Geochemistry of the host rocks of the volcanogenic massive sulfide deposit at Que River, Tasmania: Economic Geology and the Bulletin of the Society of Economic Geologists, v. 84, p. 1–21, doi:10.2113/gsecongeo.84.1.1.

Winchester, J.A., and Floyd, P.A., 1977, Geochemical discrimination of different magma series and their differentiation products using immobile elements: Chemical Geology, v. 20, p. 325–343, doi:10.1016/0009-2541(77)90057-2.

Woodhead, J., Eggins, S., and Gamble, J.A., 1993, High field strength and transition element systematics in island arc and backarc basin basalts: Evidence for multi-phase melt extraction and a depleted mantle wedge: Earth and Planetary Science Letters, v. 114, p. 491–504, doi:10.1016/0012-821X(93)90078-N.

Wu, T.-W., 1984, Geochemistry and petrogenesis of some granitoids in the Grenville province of Ontario and their tectonic implications [Ph.D. thesis]: University of Western Ontario.

You, C.-F., Castillo, P.R., Gieskes, J.M., Chan, L.H., and Spivack, A.J., 1996, Trace element behavior in hydrothermal experiments: Implications for fluid processes at shallow depths in subduction zones: Earth and Planetary Science Letters, v. 140, p. 41–52, doi:10.1016/0012-821X(96)00049-0.

Young, G.M., 2002, Geochemical investigation of a Neoproterozoic glacial unit: The Mineral Fork Formation in the Wasatch Range, Utah: Geological Society of America Bulletin, v. 114, p. 387–399, doi:10.1130/0016-7606(2002)114<0387:GIOANG>2.0.CO;2.

Zindler, A., and Hart, S.R., 1986, Chemical geodynamics: Annual Review of Earth and Planetary Sciences, v. 14, p. 493–571, doi:10.1146/annurev.ea.14.050186.002425.

Zindler, A., Staudigel, H., and Batiza, R., 1984, Isotope and trace element geochemistry of young Pacific seamounts: Implications for the scale of upper mantle heterogeneity: Earth and Planetary Science Letters, v. 70, p. 175–195, doi:10.1016/0012-821X(84)90004-9.